Risk Premia and Seasonality in Commodity Futures

Constantino Hevia
Universidad Torcuato Di Tella

Ivan Petrella
Warwick Business School and CEPR

Martin Sola
Universidad Torcuato Di Tella

March 5, 2018

Abstract

We develop and estimate a multifactor affine model of commodity futures that allows for stochastic seasonality. We document the existence of stochastic seasonal fluctuations in commodity futures and that properly accounting for the cost-of-carry curve requires at least three factors. We estimate the model using data on heating oil futures and analyze the contribution of the factors to risk premia. Correctly specifying seasonality as stochastic is important to avoid erroneously assigning those fluctuations to other risk factors. We also estimate a nonlinear version of the model that imposes the zero lower bound on interest rates and find similar results.

Keywords: Commodity futures, Seasonality, Cost-of-carry, Risk premium, Nelson and Siegel.
JEL codes: C22, G12, G13.

Acknowledgments: We thank Pavol Povala, Enrique Sentana, Ron Smith, and seminar participants at CEMFI, Universidad de Montevideo, and University of York for valuable comments. Agustin Gutierrez provided excellent research assistance.

1 Introduction

Futures prices in many energy and agricultural commodities display seasonal fluctuations. Often, those fluctuations are not perfectly predictable. From the point of view of market participants, stochastic seasonal fluctuations imply a source of risk that manifests itself in futures prices and risk premia. The purpose of this paper is to develop and estimate an affine model of futures prices that allows for stochastic variations in seasonality. We use the model to analyze the implications of stochastic seasonal fluctuations for the pricing of commodity futures and risk premia.

The earlier literature, such as Gibson and Schwartz (1990) and Litzenberger and Rabinowitz (1995), assumes that the price of commodity futures depends on two factors, a spot price factor and a cost-of-carry (or convenience yield) factor. Schwartz (1997) extends the model to include a stochastic interest rate, which became the standard three-factor model of commodity futures. Casassus and Collin-Dufresne (2005) provides a different interpretation of the three-factor model that we use to relate the cost-of-carry and the spot commodity price. Miltersen and Schwartz (1998) use the affine framework to price derivatives on commodity futures, and Hamilton and Wu (2014) study risk premia in oil futures markets. Finally, existing models of seasonal commodity futures only allow for deterministic seasonal fluctuations in prices (e.g. Sorensen, 2002) or in the cost-of-carry (e.g. Borovkova & Geman, 2006).

This paper extends the current literature in three dimensions. First, our model features stochastic seasonal fluctuations in both the spot price and the cost-of-carry. By attaching market prices of risk to seasonal factors, we are able to measure the risks associated with stochastic seasonal shocks. Second, following much of the literature on bond prices, we assume that bond yields depend on three factors. And third, consistent with data on a set of agricultural and energy commodity futures, we assume that the cost-of-carry curve is driven by three factors.

We begin with a preliminary analysis of futures prices for a group of energy and agricultural commodities that provide support to our modeling assumptions. We first document that seasonal fluctuations in this set of commodity futures are stochastic. Second, we perform a principal components analysis on the cost-of-carry curve for each commodity. We conclude that we need at least three factors to appropriately account for the dynamics of the cost-of-carry curve. The first three principal components account for 90 percent or less of the variability of the cost-of-carry

curve, with the third principal component contributing between 4 and 14 percent of the variability depending on the commodity and method used to compute the curve. Furthermore, the first principal component only accounts for between 16 and 80 percent of the variability. These results suggest that a model in which the cost-of-carry depends on a single factor misses important features of the data, and motivates our assumption that the cost-of-carry depends on three factors.

We next describe an affine model of commodity futures with stochastic seasonality in discrete time. The model prices zero-coupon bonds and commodity futures of any maturity, and stochastic variations in seasonality are driven a pair of random walks (Hannan, 1964). To estimate the model we need to impose identifying restrictions. An approach often used in the bond pricing literature is to impose identifying assumption such that the yield curve adopts an augmented Nelson and Siegel (1987) specification (Christensen, Diebold, & Rudebusch, 2011). We extend this literature to the pricing of commodity futures and find conditions under which the yield curve and the cost-of-carry curve derived from the model adopt a Nelson-Siegel representation.

We estimate the model of bond and commodity futures prices using data on U.S. zero coupon bonds and futures prices on heating oil for the period Jan-1984 through Apr-2017. We concentrate our analysis on heating oil but leave for an online supplement estimation results using data on soybeans futures. The model matches the cross-section of futures prices over time, including their seasonal pattern. We find strong evidence of stochastic seasonality: the peaks and troughs of the seasonal cycle vary over the years, and the amplitude of the seasonal fluctuations decreased over time, particularly at the end of the sample. Consistent with the theory of storage, the moderation of the estimated seasonal component coincides with a similar mitigation of the seasonal component in stocks of heating oil inventories.

Expected returns of holding a futures contract fluctuate widely over time, and most of those fluctuations come from variations in the spot, cost-of-carry, and yield curve factors. Although non-negligible, the contribution of seasonal shocks to risk premia is small. Seasonal shocks account for about 0.5 percentage points of expected returns but become less relevant at the end of our sample period. Therefore, correctly specifying seasonality in futures prices as stochastic is important mostly to avoid erroneously assigning those fluctuations to other risk factors. When we estimate the model imposing deterministic seasonality, the omitted time variation in the seasonal pattern manifests itself as large fluctuations in the cost-of-carry factors which, in turn, translate

into large and spurious fluctuations in estimated risk premia.

It is often argued that interest rate shocks have a minor impact on the time variation in commodity futures risk premia. Schwartz (1997) assumes a constant interest rate because interest rate fluctuations are orders of magnitudes lower than those in futures returns. Using the three-factor model, Casassus and Collin-Dufresne (2005) argue that the market price of interest rate shocks is barely significant. In contrast, we find that yield curve factors have a significant impact on risk premia, mostly at medium and lower frequencies. In our sample period, interest rates declined from about 12 percent to roughly zero. The contribution of interest rate factors to expected holding returns went from about -10 percentage points to 0 over the same time frame. When the slope of the yield curve is positive, long term contracts are relatively more expensive than shorter contracts while the reverse holds when the yield curve is inverted. Thus, changes in the slope of the yield curve over time affect futures prices and risk premia. Overall, we find that several measures of risk premia began to drop by 2007. This drop is associated with a decline in the risk premia associated with the commodity factors and a decline in the (negative) risk premia associated with the yield curve factors. The contribution of the seasonal shocks to risk premia also declines, but this effect is smaller than that of the other factors.

From December 2008 to December 2015, the U.S. Federal Reserve set the policy interest rate to virtually zero. We explore to what extent our results change if we explicitly impose the zero lower bound on interest rates. To that end, we adapt the yield curve model proposed by Wu and Xia (2016) and jointly estimate a model of commodity futures and bond prices that imposes the zero lower bound constraint. Although this constraint is important for bond pricing, we find that it has a minor impact on futures prices and risk premia relative to the results of the baseline model.

The paper is organized as follows. Section 2 documents two empirical regularities for commodity futures and Section 3 describes an affine model with stochastic seasonality. Section 4 proposes a representation of the model that adopts Nelson-Siegel functional forms and Section 5 describes the estimation method. Section 6 contains the main results and Section 7 concludes. Proofs are relegated to the appendix (Hevia, Petrella, and Sola (2018) contains additional material).

2 Some empirical properties of commodity futures

In this section we document two empirical regularities in a group of energy and agricultural commodity futures. The first is that seasonal fluctuations are stochastic. The second is that we need at least three factors to properly account for the variability of the cost-of-carry curve. Those results provide support to our subsequent modeling assumptions.

2.1 Stochastic seasonality in commodity futures

Futures prices in many energy and agricultural commodities display seasonal fluctuations.[1] Although it is common to model seasonality as deterministic cycles, in this section we argue that, for many commodities, those seasonal fluctuations are in fact stochastic. This distinction is important because stochastic seasonality implies an additional risk factor that affects risk premia.

Let us decompose a stochastic process $z_t = z_t^n + z_t^s$ into its seasonal (z_t^s) and non-seasonal (z_t^n) components. Deterministic seasonality can be modeled in terms of trigonometric functions,

$$z_t^s = \sum_{j=1}^{6} \left[\xi_j \cos(\tfrac{2\pi j}{12} m_t) + \xi_j^* \sin(\tfrac{2\pi j}{12} m_t) \right],$$

where $2\pi j/12$ are seasonal frequencies and ξ_j and ξ_j^* are parameters. The seasonal effect z_t^s is the sum of six deterministic cycles with periods of $12/j$ months, for $j = 1, 2, ..., 6$. The frequency $2\pi/12$ corresponds to a period of 12 months and is known as the fundamental frequency. The other frequencies represent waves with periods of less than a year.

Following Hannan (1964), we model stochastic seasonality by letting the parameters ξ_j and ξ_j^* evolve as a random walks. Thus, the stochastic seasonal component is given by

$$z_t^s = \sum_{j=1}^{6} \left[\xi_{jt} \cos(\tfrac{2\pi j}{12} m_t) + \xi_{jt}^* \sin(\tfrac{2\pi j}{12} m_t) \right], \tag{1}$$

where, $\xi_{jt} = \xi_{jt-1} + \nu_{jt}$ and $\xi_{jt}^* = \xi_{jt-1}^* + \nu_{jt}^*$ for $j = 1, 2, ..., 6$. The shocks ν_{jt} and ν_{jt}^* are orthogonal and normally distributed with variances σ_j^2 and σ_j^{*2}. When the seasonal cycle is dominated by a single seasonal peak and trough within the year (only the fundamental frequency matters), the seasonality process collapses to

$$z_t^s = \xi_t \cos(\tfrac{2\pi}{12} m_t) + \xi_t^* \sin(\tfrac{2\pi}{12} m_t), \tag{2}$$

[1] A Wald test of significance of seasonal dummies in autoregressive models of futures prices strongly reject the null of lack of seasonality for all the commodities considered below.

where ξ_t and ξ_t^* are two independent random walks.

Table 1 shows the results of three tests of the null hypothesis that seasonality in futures prices is deterministic for a number of energy commodities (gasoil, gasoline, heating oil, and natural gas) and agricultural commodities (corn, soybean, and wheat). The alternative hypothesis is that seasonal fluctuations are stochastic.[2] We use Canova and Hansen (1995) nonparametric test for parameter stability and its spectral extension developed by Busetti and Harvey (2003). The third is a parametric test also proposed by Busetti and Harvey (2003). For most commodities and contract maturities, the tests strongly reject the null hypothesis of deterministic seasonality.[3]

These results suggest that the common practice of imposing a deterministic seasonal model in commodity futures (at least for those considered here) is flawed. Moreover, deseasonalizing the data prior to any empirical analysis is also problematic for two reasons. First, extracting the seasonal component from each futures contract in isolation does not guarantee that the seasonal factors are consistent across maturities.[4] And second, by deseasonalizing the data prior to any empirical analysis one is unable to measure the contribution of seasonal shocks to risk premia. We deal with both concerns by imposing a common seasonal factor that affects futures prices of all maturities within the context of an affine model of futures prices.

2.2 Number of factors in the cost-of-carry curve

To estimate an affine model of commodity futures we need to determine the number of risk factors. Researchers agree that three factors capture most of the variation in bond yields and we follow this practice below. But less is known about the factor structure in the cost-of-carry curve. The basic model of commodity futures assumes that a single factor drives variations in the cost-of-carry. In this section we show that, in fact, we need at least three factors to properly account for the dynamics of the cost-of-carry.

A τ-period futures contract entered into at time t is an agreement to buy the commodity at time $t+\tau$ at the settlement price $F_t^{(\tau)}$. Let S_t denote the spot commodity price; $f_t^\tau = \log(F_t^{(\tau)})$, the log of the futures price; and $s_t = \log(S_t)$, the log of the spot price. The log-basis of a commodity

[2]The data are end-of-month log settlement futures prices on contracts with maturities up to 18 months ahead. Details about the sources and construction of the data are given in Hevia et al. (2018).

[3]The evidence is mixed when considering natural gas, which is often used as an example of a seasonal commodity.

[4]Hevia et al. (2018) show that seasonal patterns extracted from univariate models are not synchronized across maturities.

futures is defined as $f_t^{(\tau)} - s_t$. Following Miltersen and Schwartz (1998) and Trolle and Schwartz (2009) we *define* the cost-of-carry curve (net of bond yields) at t as the value $u_t^{(\tau)}$ (viewed as a function of maturity τ) such that the basis of the commodity futures can be written as

$$f_t^{(\tau)} - s_t = \tau(y_t^{(\tau)} + u_t^{(\tau)}), \tag{3}$$

where $y_t^{(\tau)}$ is the yield on a zero-coupon bond that matures in τ periods.

To infer the number of factors necessary to capture the variability of the cost-of-carry curve, we compute principal components of log futures prices net of the contribution of the spot, seasonal, and yield curve factors. Based on equation (3), we subtract from futures prices the contribution of bond yields and define $w_t^\tau = f_t^{(\tau)} - \tau y_t^{(\tau)}$. We use two procedures to isolate the contribution of the spot and seasonal factors. In the first, we run a series of cross-sectional regressions (one for each date) of $w_t^{(\tau)}$ on a constant and sine and cosine waves according to

$$w_t^{(\tau)} = a_{0t} + \cos\left(\tfrac{2\pi}{12}(t+\tau)\right) a_{1t} + \sin\left(\tfrac{2\pi}{12}(t+\tau)\right) a_{2t} + \epsilon_t^{(\tau)}. \tag{4}$$

The estimated constant ($\hat{a}_{0t}$) is a common shifter that affects futures prices of all maturities and captures the role of the spot factor. The coefficients associated with the sine and cosine waves ($\hat{a}_{1t}$ and $\hat{a}_{2t}$) capture the seasonal variations in the data, and the residuals $\hat{\epsilon}_t^{(\tau)}$ are an estimate of (τ times) the cost-of-carry curve. The second approach is to extract the spot and seasonal factors using standard state space techniques. We still use equation (4) but now assume that the spot factor (a_{0t}) follows a first order autoregressive process and the seasonal factors (a_{1t} and a_{2t}) follow independent random walks. We estimate the factors using the Kalman filter and construct the cost-of-carry curve using the residuals of equation (4). Finally, we perform principal components analysis on the two ways of estimating the cost-of-carry curve.

Table 2 reports the contribution of the first three principal components to the variability of the two measures of the cost-of-carry curve.[5] The result is clear: we need at least three factors to properly account for the variability of the cost-of-carry curve. The first three principal components account for about 90 percent of the variance of the cost-of-carry curve, with the third principal component explaining between 5 to 14 percent of that variance. In light of these results, we augment the traditional affine model of commodity futures by assuming that fluctuations in the cost-of-carry are driven by three factors.

[5]We extract principal components from the unbalanced panel of futures prices as in Stock and Watson (2002).

3 Affine model of commodity futures

The risk factors are represented by a vector of state variables $X_t \in \mathbb{R}^n$, that evolves as

$$X_{t+1} = \mu + \Theta X_t + \Gamma \eta_{t+1}, \tag{5}$$

where $\eta_{t+1} \sim N(0, I)$ and Γ is lower triangular. Time periods are measured in months and the state vector includes factors capturing the stochastic variation in seasonality, which we specify below.

Nominal cash flows received at time $t+1$ are priced using the stochastic discount factor

$$M_{t,t+1} = e^{-(r_t + \frac{1}{2}\Lambda_t'\Lambda_t + \Lambda_t'\eta_{t+1})} \tag{6}$$

$$\Lambda_t = \lambda_0 + \lambda_1 X_t,$$

where r_t is the one period interest rate and $\Lambda_t \in \mathbb{R}^n$ is the compensation for risk to shocks to the state vector η_{t+1}. The spot interest rate r_t is an affine function

$$r_t = \rho_0 + \rho_1' X_t, \tag{7}$$

where ρ_0 is a scalar and $\rho_1 \in \mathbb{R}^n$. Since there is no evidence of seasonality in interest rates, we set to zero the loading of ρ_1 on the seasonal factors.

3.1 Pricing government bonds

Let $P_t^{(\tau)}$ be the price of a τ-period zero-coupon bond. Absence of arbitrage implies that bond prices satisfy the pricing condition $P_t^{(\tau)} = E_t[M_{t,t+1} P_{t+1}^{(\tau-1)}]$. Using standard results (Ang & Piazzesi, 2003) one can show that log bond prices are affine functions of the risk factors

$$\log P_t^{(\tau)} = A_\tau + B_\tau' X_t, \tag{8}$$

where the scalar A_τ and the vector of loadings B_τ satisfy the recursions

$$A_\tau = A_{\tau-1} - \rho_0 + (\mu - \Gamma\lambda_0)' B_{\tau-1} + \frac{1}{2} B_{\tau-1}' \Gamma\Gamma' B_{\tau-1} \tag{9}$$

$$B_\tau = (\Theta - \Gamma\lambda_1)' B_{\tau-1} - \delta_1, \tag{10}$$

with initial conditions $A_0 = 0$ and $B_0 = 0$. The yield on a τ-period zero-coupon at date t is thus

$$y_t^{(\tau)} = -\log P_t^{(\tau)} / \tau = a_\tau + b_\tau' X_t. \tag{11}$$

3.2 Spot price and implied cost-of-carry

Consider a storable commodity with spot price S_t and with a net cost-of-carry of c_t, expressed as a continuously compounded rate of the spot price. The net cost-of-carry represents the storage and insurance costs of physically holding the commodity net of any convenience yield on inventory. It is the analog of the negative of the dividend yield of a stock and can be derived from equilibrium models such as Routledge, Seppi, and Spatt (2000).

To capture seasonality in the spot price and the cost-of-carry, we assume that their loadings on X_t are periodic functions of time. Let $\{m_t\}$ be a periodic sequence mapping the time t into the set of months $\{1, 2, ..., 12\}$. We initialize the sequence by setting $m_t = t$ for $t = 1, 2, ..., 12$, and let $m_{t+12k} = m_t$ for every t and k. We often use $\tilde{m}$ when referring to a generic month and impose the convention that $\tilde{m} + 1 = 1$ when $\tilde{m} = 12$.

Assume that the log spot commodity price is given by

$$s_t = \gamma_0 + \gamma_1^{m_t\prime} X_t, \tag{12}$$

where $\gamma_1^{m_t}$ depend on the season m_t. Since the payoff from holding the commodity between t and $t+1$ is $e^{-c_{t+1}} S_{t+1}$, the principle of no arbitrage implies that the spot price S_t satisfies

$$S_t = E_t \left[M_{t,t+1} e^{-c_{t+1}} S_{t+1} \right]. \tag{13}$$

Following Casassus and Collin-Dufresne (2005), the next proposition (proved in Hevia et al. (2018)) states that there exists an affine and seasonal cost-of-carry process c_t such that the pricing condition (13) is satisfied given the evolution of the spot price (12).

Proposition 1 (Cost-of-carry process): *The net cost-of-carry consistent with the commodity price (13) is an affine and periodic function of the state variables* $c_t = \psi_0^{m_t} + \psi_1^{m_t\prime} X_t$ *where the scalar* $\psi_0^{\tilde{m}}$ *and the vector* $\psi_1^{\tilde{m}}$ *satisfy*

$$\psi_1^{\tilde{m}+1} = \gamma_1^{\tilde{m}+1} - \left[(\Theta - \Gamma\lambda_1)^{-1} \right]' \left(\gamma_1^{\tilde{m}} + \rho_1 \right)$$

$$\psi_0^{\tilde{m}+1} = \left(\gamma_1^{\tilde{m}+1} - \psi_1^{\tilde{m}+1} \right)' (\mu - \Gamma\lambda_0) + \frac{1}{2} \left(\gamma_1^{\tilde{m}+1} - \psi_1^{\tilde{m}+1} \right)' \Gamma\Gamma' \left(\gamma_1^{\tilde{m}+1} - \psi_1^{\tilde{m}+1} \right) - \rho_0.$$

3.3 Pricing commodity futures

A τ-period futures contract entered into at time t is an agreement to buy the commodity at time $t+\tau$ at the settlement price $F_t^{(\tau)}$. Entering into a futures contract involves no initial cash-flow and a payoff of $S_{t+\tau} - F_t^{(\tau)}$ at time $t+\tau$. Therefore, if we let $M_{t,t+\tau}$ denote the stochastic discount factor for nominal payoffs received τ periods ahead, the principle of no-arbitrage implies

$$E_t\left[M_{t,t+\tau}(S_{t+\tau} - F_t^{(\tau)})\right] = 0.$$

In Appendix A we show that log-futures prices satisfy

$$f_t^{(\tau)} = C_\tau^{m_t} + D_\tau^{m_t\prime} X_t, \tag{14}$$

where $C_\tau^{\tilde{m}} = G_\tau^{\tilde{m}} - A_\tau$ and $D_\tau^{\tilde{m}} = H_\tau^{\tilde{m}} - B_\tau$, A_τ and B_τ solve equations (9) and (10), and $G_\tau^{\tilde{m}}$ and $H_\tau^{\tilde{m}}$ solve the recursions

$$G_\tau^{\tilde{m}} = G_{\tau-1}^{\tilde{m}+1} - \rho_0 + (\mu - \Gamma\lambda_0)' H_{\tau-1}^{\tilde{m}+1} + \frac{1}{2}\left(H_{\tau-1}^{\tilde{m}+1}\right)' \Gamma\Gamma' H_{\tau-1}^{\tilde{m}+1}, \tag{15}$$

$$H_\tau^{\tilde{m}} = (\Theta - \Gamma\lambda_1)' H_{\tau-1}^{\tilde{m}+1} - \rho_1, \tag{16}$$

with initial conditions $G_0^{\tilde{m}} = \gamma_0$ and $H_0^{\tilde{m}} = \gamma_1^{\tilde{m}}$ for $\tilde{m} = 1, 2, ..., 12$.[6,7];

3.4 Risk premia in commodity futures

In this section we express different notions of risk premia in terms of the components of the affine model. Since all the strategies that we consider cost zero when they are entered into, ex-ante expected return entirely reflects expected risk premia.

The *1-period log holding return* (open a position on a τ-period futures at time t and close it at time $t+1$) is $f_{t+1}^{(\tau-1)} - f_t^{(\tau)}$. The time-$t$ conditional expectation of this strategy is

$$E_t[f_{t+1}^{(\tau-1)} - f_t^{(\tau)}] = J_{\tau-1}^{m_{t+1}} + D_{\tau-1}^{m_{t+1}\prime}\Gamma\Lambda_t, \tag{17}$$

where $J_{\tau-1}^{m_{t+1}} = \frac{1}{2}[B_{\tau-1}'\Gamma\Gamma' B_{\tau-1} - H_{\tau-1}^{m_{t+1}\prime}\Gamma\Gamma' H_{\tau-1}^{m_{t+1}}]$ is a periodic Jensen inequality term. The second term, $D_{\tau-1}^{m_{t+1}\prime}\Gamma\Lambda_t$, captures the stochastic variation in expected risk premia over time.

[6] Alquist, Bauer, and Diez de los Rios (2013) study an affine model of oil futures using a setup different from ours. While we price commodity futures by discounting dollar cash flows—as usually done in the literature—they assume that there are oil denominated bonds and introduce two pricing kernels, one expressed in dollars to price dollar bonds and the other in units of oil to price oil bonds. Moreover, they do not consider seasonal fluctuations.

[7] Some authors claim that no-arbitrage restrictions only matter for the cross-section of bond yields and that they do not affect the time-series dynamics of the factors (Duffee, 2011). Nevertheless, our model has several features such as unobserved factors, stochastic seasonality, and restrictions in the physical and risk neutral measures that, when considered together, should be addressed within an arbitrage-free model.

The *spot premium* is the expected return of holding a 1-period futures contract until maturity. It is the particular case of the expected return (17) evaluated at $\tau = 1$,

$$E_t[s_{t+1} - f_t^{(1)}] = J_0^{m_{t+1}} + \gamma_1^{m_{t+1}\prime}\Gamma\Lambda_t, \tag{18}$$

where we use that a 0-period futures is equivalent to the spot price, $s_{t+1} = f_{t+1}^{(0)}$.

The *term premium* is defined as the 1-period expected holding return of a τ-period futures contract in excess of the spot premium. In terms of the affine model, the term premium is

$$E_t[(f_{t+1}^{(\tau-1)} - f_t^{(\tau)}) - (s_{t+1} - f_t^{(1)})] = J_{\tau-1}^{m_{t+1}} - J_0^{m_{t+1}} + (D_{\tau-1}^{m_{t+1}\prime} - \gamma_1^{m_{t+1}\prime})\Gamma\Lambda_t. \tag{19}$$

Another strategy is to open a position on a τ-period futures at time t and sell it as a $\tau - h$-period futures at time $t + h$. The ex-post h *-period log holding return* of this strategy can be expressed as a sum of 1-period holding returns,

$$f_{t+h}^{(\tau-h)} - f_t^{(\tau)} = [f_{t+h}^{(\tau-h)} - f_{t+h-1}^{(\tau-h+1)}] + [f_{t+h-1}^{(\tau-h+1)} - f_{t+h-2}^{(\tau-h+2)}] + ... + [f_{t+1}^{(\tau-1)} - f_t^{(\tau)}].$$

Therefore, the expected h*-period log holding return* follows from using the expected 1-period returns and the law of iterated expectations,

$$E_t[f_{t+h}^{(\tau-h)} - f_t^{(\tau)}] = \sum_{i=1}^{h} J_{\tau-i}^{m_{t+i}} + \sum_{i=1}^{h} D_{\tau-i}^{m_{t+i}\prime}\Gamma E_t[\Lambda_{t+i-1}]. \tag{20}$$

4 A representation of the affine model of commodity futures

Here we extend results in Christensen et al. (2011) to the commodity futures literature by showing that a single stochastic discount factor can be used to simultaneously price bonds and commodity futures displaying stochastic seasonality in such a way that the yield curve and the cost-of-carry curve adopt augmented Nelson and Siegel functional forms. This representation of the model is simple yet flexible enough to match the different shapes of the cost-of-carry and yield curves.

We first write the log-basis (3) emphasizing the contribution of the seasonal factors as,

$$f_t^{(\tau)} = \beta_{0t} + \tau(y_t^{(\tau)} + \tilde{u}_t^{(\tau)}) + e^{-\omega\tau}\left[\xi_t \cos(\tfrac{2\pi}{12} m_{t+\tau}) + \xi_t^* \sin(\tfrac{2\pi}{12} m_{t+\tau})\right], \tag{21}$$

where we interpret β_{0t} as the deseasonalized spot commodity factor and $\tilde{u}_t^{(\tau)}$ as the cost-of-carry curve net of any *stochastic* seasonal component.[8] The last term on the right side reflects the

[8] Hevia et al. (2018) show that the pair of seasonal factors associated with the fundamental frequency is enough to characterize seasonality in heating oil and soybean futures. Thus, from now on we assume that seasonal fluctuations follow the process (2).

contribution of the seasonal factors to futures prices of different maturities. When $\tau = 0$ the futures price is the spot commodity price and equation (21) becomes

$$s_t = \beta_{0t} + \xi_t \cos(\tfrac{2\pi}{12} m_t) + \xi_t^* \sin(\tfrac{2\pi}{12} m_t). \tag{22}$$

To extract the seasonality of a futures contract with τ months to maturity, we compute the expected seasonal component at time $t+\tau$ conditional on information at time t, and then multiply the resulting expression by a discounting factor $e^{-\omega\tau}$.

There is agreement in the bond pricing literature that three factors are sufficient to summarize the evolution of the yield curve over time. Thus, we parametrize the yield curve $y_t^{(\tau)}$ using a dynamic Nelson and Siegel model as in Christensen et al. (2011),

$$y_t^{(\tau)} = a_\tau + \delta_{1t} + \left(\frac{1-e^{-\zeta_1\tau}}{\zeta_1\tau}\right)\delta_{2t} + \left(\frac{1-e^{-\zeta_1\tau}}{\zeta_1\tau} - e^{-\zeta_1\tau}\right)\delta_{3t}, \tag{23}$$

where δ_{1t}, δ_{2t}, and δ_{3t} are latent variables interpreted as level, slope and curvature factors, and the parameter ζ_1 determines the shape of the loadings on the factors δ_{2t} and δ_{3t}.

Section 2 shows that we need at least three factors to properly characterize the non-seasonal component of the cost-of-carry curve $\tilde{u}_t^{(\tau)}$. Therefore, we also look for conditions under which the cost-of-carry curve adopts an augmented dynamic Nelson and Siegel form,

$$\tilde{u}_t^{(\tau)} = g_\tau^{m_t} + \beta_{1t} + \left(\frac{1-e^{-\zeta_2\tau}}{\zeta_2\tau}\right)\beta_{2t} + \left(\frac{1-e^{-\zeta_2\tau}}{\zeta_2\tau} - e^{-\zeta_2\tau}\right)\beta_{3t}, \tag{24}$$

where β_{1t}, β_{2t}, and β_{3t} are level, slope, and curvature factors. Even though $\tilde{u}_t^{(\tau)}$ is independent of seasonal shocks, rendering the Nelson and Siegel parametrization arbitrage-free still requires the term $g_\tau^{m_t}$ to depend on the season (month) m_t, although in a deterministic fashion.

We now show that Nelson and Siegel parametrization belongs to the family of affine models described in Section 3. Although it is known that one can impose restrictions on an affine model of bond prices to obtain a Nelson and Siegel representation of the yield curve (Christensen et al., 2011), the extension to the commodity futures literature has not been proved so far.

The vector of risk factors is $X_t = [\delta_{1t}, \delta_{2t}, \delta_{3t}, \beta_{0t}, \beta_{1t}, \beta_{2t}, \beta_{3t}, \xi_t, \xi_t^*]'$. Our task is to find parameters λ_0, λ_1, ρ_0, ρ_1, γ_0, and $\gamma_1^{m_t}$ such that the yield curve and the cost-of-carry curve adopt the functional forms (23) and (24). These conditions are summarized in

Proposition 2 (Nelson and Siegel representation): *Consider parameters of the risk-neutral measure*

$$\Theta^{Q} = \begin{bmatrix} 1 & 0 & 0 & 0 & 0 & 0 & 0 & 0 & 0 \\ 0 & e^{-\zeta_1} & \zeta_1 e^{-\zeta_1} & 0 & 0 & 0 & 0 & 0 & 0 \\ 0 & 0 & e^{-\zeta_1} & 0 & 0 & 0 & 0 & 0 & 0 \\ 1 & \frac{1-e^{-\zeta_1}}{\zeta_1} & \frac{1-e^{-\zeta_1}}{\zeta_1} - e^{-\zeta_1} & 1 & 1 & \frac{1-e^{-\zeta_2}}{\zeta_2} & \frac{1-e^{-\zeta_2}}{\zeta_2} - e^{-\zeta_2} & 0 & 0 \\ 0 & 0 & 0 & 0 & 1 & 0 & 0 & 0 & 0 \\ 0 & 0 & 0 & 0 & 0 & e^{-\zeta_2} & \zeta_2 e^{-\zeta_2} & 0 & 0 \\ 0 & 0 & 0 & 0 & 0 & 0 & e^{-\zeta_2} & 0 & 0 \\ 0 & 0 & 0 & 0 & 0 & 0 & 0 & e^{-\omega} & 0 \\ 0 & 0 & 0 & 0 & 0 & 0 & 0 & 0 & e^{-\omega} \end{bmatrix}$$

and $\mu^{Q} \in R^{n}$, *where* $\zeta_1, \zeta_2, \omega > 0$. *Let* $\lambda_0 = \Gamma^{-1}\left(\mu - \mu^{Q}\right)$, $\lambda_1 = \Gamma^{-1}\left(\Theta - \Theta^{Q}\right)$, $\rho_0 = 0$, $\gamma_0 = 0$,

$$\rho_1 = \left[1, \tfrac{1-e^{-\zeta_1}}{\zeta_1}, \tfrac{1-e^{-\zeta_1}}{\zeta_1} - e^{-\zeta_1}, 0, 0, 0, 0, 0, 0\right]', \text{ and}$$

$$\tilde{\gamma}_1 = \left[0, 0, 0, 1, 0, 0, 0, \cos(\tfrac{2\pi}{12}\tilde{m}), \sin(\tfrac{2\pi}{12}\tilde{m})\right]'$$

for $\tilde{m} = 1, 2, ..., 12$. *Then, the yields and futures prices adopt the parametrization (21), (23), and (24).*

5 Estimation method

We estimate the model by maximum likelihood using the Kalman filter to evaluate the prediction error decomposition of the likelihood function and to handle missing observations, a common feature in the market of commodity futures. The state variables follow the process (5), and the observation equation consists of futures prices and bond yields that satisfy equations (11) and (14) augmented with measurement errors $\varepsilon_{yt}^{(\tau_y)}$ and $\varepsilon_{ft}^{(\tau_f)}$,

$$y_t^{(\tau_y)} = a_{\tau_y} + b'_{\tau_y} X_t + \varepsilon_{yt}^{(\tau_y)}. \tag{25}$$

$$f_t^{(\tau_f)} = C_{\tau_f}^{m_t} + D_{\tau_f}^{m_t\prime} X_t + \varepsilon_{ft}^{(\tau_f)} \tag{26}$$

Bond yields are observed for a set of maturities $\tau_y \in \mathcal{T}_y$ and futures prices may be observed for a different set of maturities $\tau_f \in \mathcal{T}_f$. We use bond yields for maturities up to 5 years to properly estimate the shape of the yield curve and futures contracts with maturities from 1 to 18 months.

The intercept and factor loadings satisfy the functional forms (21), (23), and (24). Namely, $C_\tau^{m_t} = G_\tau^{m_t} - A_\tau$, $D_\tau^{m_t} = H_\tau^{m_t} - B_\tau$, $a_\tau = -A_\tau/\tau$, $b_\tau = -B_\tau/\tau$,

$$H_\tau^{m_t} = \left[0, 0, 0, 1, \tau, \tfrac{1-e^{-\zeta_2\tau}}{\zeta_2}, \tfrac{1-e^{-\zeta_2\tau}}{\zeta_2} - \tau e^{-\zeta_2\tau}, e^{-\omega\tau}\cos(\tfrac{2\pi}{12}(m_t+\tau)), e^{-\omega\tau}\sin(\tfrac{2\pi}{12}(m_t+\tau))\right]',$$

$$B_\tau = \left[-\tau, -\tfrac{1-e^{-\zeta_1\tau}}{\zeta_1}, -\left(\tfrac{1-e^{-\zeta_1\tau}}{\zeta_1} - \tau e^{-\zeta_1\tau}\right), 0, 0, 0, 0, 0, 0\right]',$$

and A_τ and $G_\tau^{m_t}$ satisfy (9) and (15). In addition, stochastic seasonality enters into equation (26) as periodic loading on the factors ξ_t and ξ_t^*.[9]

6 Empirical results

We estimate two versions of the model: one with stochastic seasonaliy (SS) and one with deterministic seasonality (DS).[10] In this section we focus on the case of heating oil futures. (Hevia et al. (2018) show results for soybean futures.)

Table 3 reports the estimates of the model with stochastic seasonality.[11] The Akaike information criterion favors the model with stochastic seasonality (-102383 versus -97850), and the Scharwz and Hannan-Quinn criteria give similar results. The estimated commodity factors in the SS model are radically different from those in the DS model (Figure 1), with the cost-of-carry factors showing clear signs of seasonality in the latter but not in the former.[12] Furthermore, the SS model also dominates the DS model in terms of pricing errors (Table 4).

Figure 2 (top panel) displays the estimated seasonal components. The seasonal peak is attained at the beginning of the winter season and the trough, at the beginning of the summer season. The peaks and troughs of the seasonal pattern in the SS model change over time (possibly depending on the severity of the winter season) and there is a drop in seasonal fluctuations at the end of the sample. This drop may be due to a change in the composition of demand: while the residential use of heating oil has decreased (which is mostly seasonal) and exports increased, its use as transportation fuel has increased over time (a mostly non-seasonal use).[13] Moreover, this finding

[9] Since $\mu^{Q\prime} D_{\tau-1}$ is a scalar, we can only identify a single parameter in $\mu^{Q\prime}$. We thus set $\mu^Q = [\mu_1^Q, 0, 0, 0, 0, 0, 0, 0]'$. Also, note that ζ_1 and ζ_2 are identified because ζ_2 appears only in equation (26) while ζ_1 appears in both, (25) and (26).

[10] In the model with deterministic seasonality we set $\sigma_\xi = \sigma_{\xi^*} = 0$ and estimate ξ_0 and ξ_0^* as free parameters.

[11] Hevia et al. (2018) contains the estimates of the model with deterministic seasonality.

[12] The estimated matrix $\widehat{\Theta}_{\beta\beta}$ in the DS model contains complex roots corresponding to a cycle of about 12 months.

[13] According to EIA (2017), the share of heating oil consumption for residential use has decreased by more than two thirds from the beginning to the end of the sample, while the share of transportation distillate use increased by over

is also consistent with anecdotal evidence suggesting a vanishing seasonality in oil prices.[14] As a result, the DS model underestimates the seasonality at the beginning of the sample and over estimates it at the end of it.

The model with deterministic seasonality also distorts the estimated factors (Figure 1). The DS model is unable capture all seasonal fluctuations from futures prices and erroneously attributes those cycles to fluctuations in the cost-of-carry factors. Moreover, since β_{1t} and β_{2t} determine the variations of the cost-of-carry curve at the short and long end of the curve, spurious fluctuations in these factors lead to spurious fluctuations in estimated risk premia.

The shape of the cost-of-carry curve depends on the parameter ζ_2, which is more than twice as large in the model with stochastic seasonality (0.416 versus 0.197). The parameter ζ_2 also determines the evolution of the risk factors under the risk-neutral measure and, therefore, the associated market prices of risk. The lower is ζ_2, the higher is the persistence of the level and slope factors β_{1t} and β_{2t} under the risk-neutral measure, and the lower is the impact of the past curvature β_{3t} on the current slope β_{2t}. The estimated ζ_2 in the model with deterministic seasonality implies more persistent factors and a weaker relation between the lagged curvature and the current slope. Therefore, the seasonal cycles leaked into the estimated cost-of-carry factors affect the dynamics of risk premia.

Finally, the model with stochastic seasonality is able to match the different shapes of the futures curve observed in our sample (Figure 3). On some dates, it is not even clear whether the futures curve is upward sloping or inverted unless one strips out the seasonal component. Furthermore, the amplitude of the seasonal factor depends on the particular dates that we choose. This observation is inconsistent with the predictions of a model with deterministic seasonality.

6.1 Seasonality and the theory of storage

It is of interest to determine the source of the moderation of the seasonal component. The theory of storage relates the stock of inventories with the cost-of-carry.[15] We compare the seasonal

50% over the same period. Moreover, the U.S. distillate exports grew to 1.5 million b/d in 2017, whereas they had been stable around 0.2 million b/d from the beginning of our sample up to the end of 2005.

[14] For instance, the U.S. Energy Information Administration (EIA, 2013) notes that *"looking at data for the last 13 years, it is apparent that the traditional northern hemisphere winter spike in demand [for oil] has become increasingly less pronounced."*

[15] In the traditional model, the convenience yield measures the option value of holding inventories when there is a positive probability of stock-outs (Deaton & Laroque, 1992; Gorton, Hayashi, & Rouwenhorst, 2013; Routledge et al., 2000). However, the relation between inventories and convenience yields also exists without stock-outs but allowing for

component extracted from data on heating oil inventories with the estimated seasonal component of the affine model. The bottom left panel of Figure 2 shows a striking similarity between the two series: the peaks and troughs are well aligned and the decline in the amplitude of the seasonal components is similar in the two series. This result suggests that the moderation in seasonal components of heating oil prices is capturing the same phenomenon in the stock of heating oil inventories. Furthermore, also consistent with the theory of storage, the estimated level factor of the cost-of-carry β_{1t} is highly correlated with the non-seasonal component of the stock of heating oil inventories (bottom right panel of Figure 2).

6.2 Risk premia in heating oil futures markets

Since entering into a futures contract costs zero, any expected return is a risk premium. Here we analyze the risk associated with holding futures contracts for one period and that associated with holding the contract to maturity. We find that risk premia in heating oil futures markets declined over time and that it has been positive on average until 2005 and negative afterwards. The change in the risk premium coincides with an abrupt increase in heating oil spot prices and with an increased participation by financial investors in commodity futures markets.[16] In addition, we find that the contribution of the spot, cost-of-carry, and yield curve factors to the time variation of risk premia is substantial, while seasonal factors play a modest role.

Figure 4 shows the 1-month expected holding return for futures contracts that mature in 1 month and 18 months ahead. Commodity factors (spot and cost-of-carry) explain most of the evolution of risk premia. Yet, the contribution of the yield curve factors is also substantial, particularly at the beginning of the sample when interest rates are high. As interest rates drop over time, so does the importance of the yield curve factors. The contribution of the seasonal shocks is about 0.6 percentage points at the beginning of the sample and becomes smaller as the seasonal component gets smaller over time (Figure 2)

other frictions in the production and storage process, such as adjustment costs (Evans & Guthrie, 2017). Since we do not aim to identify the precise interpretation of this relation, any of those models could be consistent with the observed relation.

[16]The increased entry of non-commercial traders coincides with an increase in open interest and trading volume over the last decade. The EIA reports that the average daily volume of futures contracts on petroleum products was four time larger in 2017 than the 2000-2006 average (see https://www.eia.gov/finance/markets/products/financial_markets.php). Hamilton and Wu (2014) document a similar shift in crude oil risk premia in 2005 and also attribute it to the entry of non-commercial traders into that market.

The estimated loading of expected returns on the yield curve level factor (δ_{1t}) is negative and its importance increases with the maturity of the contract. Furthermore, the loading on the slope factor (δ_{2t}) is positive when the yield curve is upward sloping, negative when the yield curve is inverted, and its importance decreases for longer maturity contracts. The upper right panel of Figure 4 is consistent with those observations. The contribution of the yield curve factors to the risk premium of the 18-months futures contract tracks closely the negative of the level factor (δ_{1t}), while that of the 1-month contract is smoother and highly correlated with the slope factor (δ_{2t}).

The bottom left panel of the figure shows that commodity factors are very volatile and that their impact on risk premia is large. It shows that the importance of the cost-of-carry level factor (β_{1t}) increases with the maturity of the contract and that this factor is highly and negatively correlated with the component of expected return accounted for by the commodity factors (-0.82 and -0.76 for the 18-month and 1-month contracts, respectively).

Figure 5 displays the expected risk premia of holding a 18 months futures contracts during 1 and 18 months. As the holding period increases, the owner of the contract is exposed to longer term risks. As a result, the spot commodity factor (β_{0t}) and the slope factor of the yield curve (δ_{2t}) become more relevant risk factors. For instance, during periods of inverted yield curves, shorter term futures contracts tend to be more valuable than longer term contracts (equation 3). Therefore, expected returns of longer term contracts increase.

The upper right panel of Figure 5 shows that the contribution of the slope yield curve factor increases with the holding period: long holding returns tend to follow more closely the slope of the yield curve than short holding returns. Moreover, periods with inverted yield curves are roughly associated with higher total expected risk premia (top panels). In addition, the bottom left panel shows that the contribution of the commodity factors tends to follow the short and medium term movements of the spot commodity factor. Interestingly, the longer term movements are negatively correlated: periods when the spot factor is relatively high are periods when expected risk premia is negative.

6.3 The zero lower bound on interest rates

From December 2008 to December 2015, the U.S. Federal Reserve set the policy interest rate to 0.25 percentage points, virtually hitting the zero lower bound (ZLB) on interest rates. If one imposes

the ZLB constraint, the model ceases to be affine in the risk factor, which causes analytical and econometric challenges. In this section we explore to what extent our results are distorted by ignoring the ZLB on interest rates.

The model is similar to that described in Section 3 but replacing the interest rate process (7) by an affine shadow interest rate of the form

$$z_t = \rho_0 + \rho_1' X_t.$$

The short term interest rate is the maximum of the shadow rate z_t and a lower bound $\underline{r} = 0$,

$$r_t = \max(z_t, \underline{r}).$$

The stochastic discount factor and the market prices of risk are still given by equations (5) and (6), and the parameters λ_0 and λ_1 still satisfy the restrictions imposed in Proposition 2.

This modification renders the model non-linear. While we could approximate the solution using numerical techniques, estimating the parameters becomes challenging because each evaluation of the likelihood function requires numerically solving the model and performing an non-linear filtering procedure. Instead, we adapt the methodology proposed by Wu and Xia (2016) and use an approximate solution whereby the yield on a τ-period zero coupon bond can be written as

$$y_t^{(\tau)} = \underline{r} + \frac{1}{\tau}\sum_{j=0}^{\tau} \sigma_j^Q g\left(\frac{\tilde{a}_j + \tilde{b}_j' X_t - \underline{r}}{\sigma_j^Q}\right). \tag{27}$$

Here, $\tilde{a}_j = \rho_0 + \rho_1'\left(\sum_{i=0}^{j-1}\Theta^{Qi}\right)\mu^Q - 0.5\rho_1'\left(\sum_{i=0}^{j-1}\Theta^{Qi}\right)\Gamma\Gamma'\left(\sum_{i=0}^{j-1}\Theta^{Qi}\right)'\rho_1$; $\tilde{b}_j' = \rho_1'(\Theta^Q)^j$; $\sigma_j^Q = \left[\rho_1'\left(\sum_{i=0}^{j-1}(\Theta^{Qi})\Gamma\Gamma'(\Theta^{Qi})'\right)\rho_1\right]^{1/2}$; and $g(x) = x\Phi(x) + \phi(x)$, where Φ is the standard normal cumulative distribution and ϕ is the associated density.[17] The function $g(x)$ is non-negative, increasing, approaches zero as x decreases, and approaches $g(x) = x$ as x increases.

Let $y_t^{(\tau)} = y^{(\tau)}(X_t)$, where $y^{(\tau)}(X_t)$ is defined as the right side of equation (27). With this notation, the observation equations of the state-space system are

$$\begin{aligned} y_t^{(\tau_y)} &= y^{(\tau_y)}(X_t) + \varepsilon_{yt}^{(\tau_y)} \\ f_t^{(\tau_f)} &= \beta_{0t} + \tau_f\left(y^{(\tau_f)}(X_t) + \tilde{u}_t^{(\tau_f)}\right) + e^{-\omega\tau}\left[\xi_t \cos(\tfrac{2\pi}{12}m_{t+\tau}) + \xi_t^* \sin(\tfrac{2\pi}{12}m_{t+\tau})\right] + \varepsilon_{ft}^{(\tau_f)}, \end{aligned} \tag{28}$$

where $\varepsilon_{yt}^{(\tau_y)}$ and $\varepsilon_{ft}^{(\tau_f)}$ are measurement errors, $\tau_y \in \mathcal{T}_y$, $\tau_f \in \mathcal{T}_f$, and $\tilde{u}_t^{(\tau_f)}$ is given by equation

[17] Hevia et al. (2018) contains a detailed description of the model and the estimation procedure. Wu and Xia (2016) actually solve the model in terms of one-period forward interest rates. To make it comparable with the previous section, we chose to compute bond yields by adding one-period forward interest rates.

(24). As before, the state variables evolve according to equation (5). To estimate the parameters of the model, we use the the extended Kalman filter to evaluate the likelihood function. Details of the algorithm and the estimated parameters are described in Hevia et al. (2018).

Figure 6 compares results from the affine model with those of the model that imposes the ZLB on interest rates. The upper left panel displays the short term interest rate r_t in the baseline model and the shadow interest rate imposing the ZLB. Both lines are almost identical except between mid-2013 and the end of 2015, when the shadow rate becomes negative while the short rate in the baseline model is roughly zero. The upper right and middle left panels compare the level and slope yield curve factors (δ_{1t} and δ_{2t}). Again they are very similar even during the zero lower bound period. The curvature factor (δ_{3t}) differs between models but it only explains a negligible fraction of the variation in bond yield and risk premia. The level factors of the cost-of-carry (β_{1t}) are indistinguishable even during the zero lower bound period (middle right panel). Although not shown in the figure, the same pattern is true for the other cost-of-carry factors (β_{2t} and β_{3t}), the spot factor β_{0t}, and the seasonal factors ξ_t and ξ_t^*. Lastly, the bottom panels display the spot premium and the expected return from holding an 18 months contract to maturity. Both measures of risk premia are very similar between models and their pairwise correlation is 0.97 for the former and over 0.99 for the latter.

From these results we conclude that the baseline model performs very well even during the periods in which the interest rates were at the zero lower bound. The commodity factors, which are the main drivers of risk premia, are virtually identical in both models. This is because the periods in which interest rate factors differ the most (when the ZLB is binding) are precisely those periods in which changes in interest rates have the lowest impact on futures prices (equation (28)).

6.4 Decomposing risk premia during the 1997-1998 oil price shock

We now look at the evolution of the futures curve, and the spot and term premiums around the 1997-1998 oil price shock. This was a period with large movements in commodity prices that is particularly interesting because the futures curve was in backwardation before the 1997 peak and in contango at the 1998 trough. Falling oil prices were associated with the emergence of a contango in the futures market which lead to the usual time spread strategies (long a futures contract and short a contract with a different maturity).

To assess the risk inherent in time spread strategies, it is useful to decompose the expected 1-month holding return of a τ-period contract into a spot premium (expected return of holding a 1-month contract) and a term premium (expected 1-month return of a τ-period contract in excess of that of a 1-month contract),

$$\underbrace{E_t[f_{t+1}^{(\tau-1)} - f_t^{(\tau)}]}_{\text{1-month expected holding return}} = \underbrace{E_t[s_{t+1} - f_t^{(1)}]}_{\text{spot premium}} + \underbrace{E_t[(f_{t+1}^{(\tau-1)} - s_{t+1}) + (f_t^{(1)} - f_t^{(\tau)})]}_{\text{term premium}}.$$

Heating oil prices reached a peak in January 1997 and the associated spot premium was large and positive (Figure 7). The reason is that periods of backwardation are usually associated with drop in stocks of heating oil inventories and increases in the spot price. In the 1998 trough, the spot premium was negative and large, consistent with the futures curve being in contango, accumulation of inventories, and an expected fall in the spot price.

The risk inherent in the abnormally high commodity price of 1997 was reflected in a negative and decreasing term premium (top left panel). As prices were too high, investors demanded a lower premium to hold long contracts because they expected an eventual drop in the price and, hence, were willing to accept a negative premium. In effect, the downward sloping futures curve of January 1997 reflected the expectation of lower spot price in the future. The futures curve switched from backwardation to contango in April 1997 while at the 1998 trough, as heating oil prices were expected to recover, the term premium turned positive and hump-shaped as investors demanded a positive premium for holding long dated contracts.

7 Concluding remarks

In this paper we document that seasonal fluctuations in futures contracts for a group of energy and agricultural commodities are stochastic. In addition, we show evidence that properly accounting for the variability in the cost-of-carry curve for the same group of commodities requires of at least three factors. These observations motivate the main contribution of the paper: developing and estimating a multifactor affine model of commodity futures and bond prices that allows for stochastic variations in seasonality. We show that there is single pricing kernel that prices bonds and commodity futures in such a way that the yield curve and the cost-of-carry curve adopt Nelson-Siegel functional forms.

We estimate the model using data on heating oil futures and U.S. bond prices. We observe a decline in the amplitude of seasonal fluctuations in the futures prices that coincides with a similar moderation in the amplitude of the seasonal pattern of stocks of heating oil inventories. This observation is consistent with the theory of storage. Next, we measure the contribution of the different factors to risk premia. We find that most high frequency fluctuations in risk premia are due to variations in the spot price factor and other factors associated with the cost-of-carry curve. Correctly specifying seasonality in futures prices as stochastic is important mostly to avoid erroneously assigning those fluctuations to other risk factors. In addition, in contrast with usual claims in the literature, we find that factors associated with bond yields have a significant contribution to risk premia in commodity futures, mostly at medium and lower frequencies.

Finally, we estimate a non-linear version of the model that imposes the zero lower bound on interest rates. Although the zero lower bound constraint is important for bond pricing, it has a minor impact on futures prices and risk premia.

References

Alquist, R., Bauer, G. H., & Diez de los Rios, A. (2013). *Macroeconomic drivers of crude oil futures risk premia* (Tech. Rep.). Bank of Canada.

Ang, A., & Piazzesi, M. (2003). A no-arbitrage vector autoregression of term structure dynamics with macroeconomic and latent variables. *Journal of Monetary Economics*, *50*(4), 745-787.

Borovkova, S., & Geman, H. (2006). Seasonal and stochastic effects in commodity forward curves. *Review of Derivatives Research*, *9*(2), 167-186.

Busetti, F., & Harvey, A. (2003). Seasonality Tests. *Journal of Business & Economic Statistics*, *21*(3), 420-36.

Canova, F., & Hansen, B. E. (1995). Are Seasonal Patterns Constant over Time? A Test for Seasonal Stability. *Journal of Business & Economic Statistics*, *13*(3), 237-52.

Casassus, J., & Collin-Dufresne, P. (2005). Stochastic convenience yield implied from commodity futures and interest rates. *Journal of Finance*, *60*(5), 2283-2331.

Christensen, J. H., Diebold, F. X., & Rudebusch, G. D. (2011). The affine arbitrage-free class of Nelson-Siegel term structure models. *Journal of Econometrics*, *164*(1), 4-20.

Deaton, A., & Laroque, G. (1992). On the behaviour of commodity prices. *Review of Economic Studies*, *59*(1), 1-23.

Duffee, G. (2011). *Forecasting with the term structure: The role of no-arbitrage restrictions* (Economics Working Paper Archive No. 576). The Johns Hopkins University,Department of Economics.

EIA. (2013). *Oil market report.* (Tech. Rep.). Retrieved from https://www.iea.org/media/omrreports/fullissues/2013-12-11.pdf

EIA. (2017). *Seasonal swings in u.s. distillate inventories lower as consumption patterns change* (Today in Energy). Retrieved from https://www.eia.gov/todayinenergy

Evans, L., & Guthrie, G. (2017). Commodity Prices and the Option Value of Storage. In *Real Options in Energy and Commodity Markets* (p. 3-29). World Scientific Publishing Co. Pte. Ltd.

Gibson, R., & Schwartz, E. S. (1990). Stochastic convenience yield and the pricing of oil contingent claims. *Journal of Finance*, *45*(3), 959-76.

Gorton, G. B., Hayashi, F., & Rouwenhorst, K. G. (2013). The Fundamentals of Commodity Futures Returns. *Review of Finance*, *17*(1), 35-105.

Hamilton, J. D., & Wu, J. C. (2014). Risk premia in crude oil futures prices. *Journal of International Money and Finance*, *42*(C), 9-37.

Hannan, E. J. (1964). The estimation of a changing seasonal pattern. *Journal of the American Statistical Association*, *59*(308), 1063-1077.

Hevia, C., Petrella, I., & Sola, M. (2018). *Supplement to "risk premia and seasonality in commodity futures* (Working Paper). Universidad Torcuato Di Tella.

Hong, Z., Niu, L., & Zeng, G. (2016). *Discrete-time arbitrage-free nelson-siegel term structure model and application* (WISE Working Paper).

Joslin, S., Singleton, K., & Zhu, H. (2011). A new perspective on gaussian dynamic term structure models. *Review of Financial Studies*, *24*(3), 926-970.

Litzenberger, R. H., & Rabinowitz, N. (1995). Backwardation in Oil Futures Markets: Theory and Empirical Evidence. *Journal of Finance*, *50*(5), 1517-45.

Miltersen, K. R., & Schwartz, E. S. (1998). Pricing of options on commodity futures with stochastic term structures of convenience yields and interest rates. *Journal of Financial and Quantitative Analysis*, *33*(01), 33-59.

Nelson, C. R., & Siegel, A. F. (1987). Parsimonious Modeling of Yield Curves. *The Journal of*

Business, *60*(4), 473-89.

Routledge, B. R., Seppi, D. J., & Spatt, C. S. (2000). Equilibrium Forward Curves for Commodities. *Journal of Finance*, *55*(3), 1297-1338.

Schwartz, E. S. (1997). The stochastic behavior of commodity prices: Implications for valuation and hedging. *Journal of Finance*, *52*(3), 923-73.

Sorensen, C. (2002). Modeling seasonality in agricultural commodity futures. *Journal of Futures Markets*, *22*(5), 393-426.

Stock, J., & Watson, M. (2002). Forecasting Using Principal Components From a Large Number of Predictors. *Journal of the American Statistical Association*, *97*, 1167-1179.

Trolle, A. B., & Schwartz, E. S. (2009). Unspanned Stochastic Volatility and the Pricing of Commodity Derivatives. *Review of Financial Studies*, *22*(11), 4423-4461.

Wu, J. C., & Xia, F. D. (2016). Measuring the macroeconomic impact of monetary policy at the zero lower bound. *Journal of Money, Credit and Banking*, *48*(2-3), 253–291.

A Appendix: Proofs

Rewrite the pricing condition of a futures contract that matures in τ periods as

$$F_t^{(\tau)} E_t[M_{t,t+1}] = E_t[M_{t,t+\tau} S_{t+\tau}]. \tag{A.1}$$

The price of a contract written at time $t+1$ with settlement date at $t+\tau$ is

$$F_{t+1}^{(\tau-1)} E_{t+1}[M_{t+1,t+\tau}] = E_{t+1}[M_{t+1,t+\tau} S_{t+\tau}].$$

Multiply both sides of this expression by $M_{t,t+1}$, use $M_{t,t+1} M_{t+1,t+\tau} = M_{t,t+\tau}$, and take expectations conditional on information at time t to obtain

$$E_t[M_{t,t+\tau} S_{t+\tau}] = E_t\left[M_{t,t+1} F_{t+1}^{(\tau-1)} E_{t+1}[M_{t+1,t+\tau}]\right].$$

Using this equation into (A.1), and noting that $E_t[M_{t,t+\tau}] = P_t^{(\tau)}$ and $E_t[M_{t+1,t+\tau}] = P_{t+1}^{(\tau-1)}$ gives

$$V_t^{(\tau)} = E_t[M_{t,t+1} V_{t+1}^{(\tau-1)}], \tag{A.2}$$

where $V_t^{(\tau)} = F_t^{(\tau)} P_t^{(\tau)}$. Conjecture a solution of the form $\log V_t^{(\tau)} = G_\tau^{m_t} + H_\tau^{m_t\prime} X_t$. Using equations (5) and (6) into (A.2), and evaluating the conditional expectation gives

$$G_\tau^{m_t} + H_\tau^{m_t\prime} X_t = G_{\tau-1}^{m_{t+1}} + H_{\tau-1}^{m_{t+1}\prime}(\mu - \Gamma\lambda_0) + \tfrac{1}{2} H_{\tau-1}^{m_{t+1}\prime} \Gamma\Gamma' H_{\tau-1}^{m_{t+1}} - \rho_0 + \left(H_{\tau-1}^{m_{t+1}\prime}(\Theta - \Gamma\lambda_1) - \rho_1'\right) X_t.$$

Fix a month $\tilde{m}$ and match coefficients to obtain

$$G_\tau^{\tilde{m}} = G_{\tau-1}^{\tilde{m}+1} + H_{\tau-1}^{\tilde{m}+1\prime}(\mu - \Gamma\lambda_0) + \tfrac{1}{2}H_{\tau-1}^{\tilde{m}+1\prime}\Gamma\Gamma' H_{\tau-1}^{\tilde{m}+1} - \rho_0,$$
$$H_\tau^{\tilde{m}} = (\Theta - \Gamma\lambda_1)' H_{\tau-1}^{\tilde{m}+1} - \rho_1,$$

Also, note that $V_t^{(0)} = F_t^{(0)} = S_t$. Therefore, the conjecture and equation (12) imply

$$G_0^{m_t} + H_0^{m_t\prime} X_t = \gamma_0 + \gamma_1^{m_t\prime} X_t.$$

Thus, $G_0^{\tilde{m}} = \gamma_0$ and $H_0^{\tilde{m}} = \gamma_1^{\tilde{m}}$ for $\tilde{m} = 1, 2, ..., 12$. Finally, note that

$$f_t^\tau = \log(V_t^{(\tau)}/P_t^{(\tau)}) = G_\tau^{m_t} - A_\tau + (H_\tau^{m_t} - B_\tau)' X_t.$$

Equation (14) follows by setting $C_\tau^{m_t} = G_\tau^{m_t} - A_\tau$ and $D_\tau^{m_t} = H_\tau^{m_t} - B_\tau$.

Proof of Proposition 2. Nelson and Siegel representation.

Log-bond prices and log-futures prices are affine functions of the state $p_t^{(\tau)} = A_\tau + B_\tau' X_t$ and $f_t^{(\tau)} = C_\tau^{\tilde{m}} + D_\tau^{\tilde{m}\prime} X_t$. Given the proposed parameters of the affine model, set $B_0 = \mathbf{0}$ and $H_0^{\tilde{m}} = \gamma_1^{\tilde{m}}$, and let the factor loadings B_τ and $H_\tau^{\tilde{m}}$ satisfy the recursions

$$B_\tau = \Theta^{Q\prime} B_{\tau-1} - \rho_1 \tag{A.3}$$
$$H_\tau^{\tilde{m}} = \Theta^{Q\prime} H_{\tau-1}^{\tilde{m}+1} - \rho_1, \tag{A.4}$$

and define $C_\tau^{\tilde{m}} = G_\tau^{\tilde{m}} - A_\tau$ and $D_\tau^{\tilde{m}} = H_\tau^{\tilde{m}} - B_\tau$. Now partition the matrix Θ^Q as

$$\Theta^Q = \begin{bmatrix} \Theta^Q_{\delta\delta} & \Theta^Q_{\delta\beta} & \Theta^Q_{\delta\xi} \\ \Theta^Q_{\beta\delta} & \Theta^Q_{\beta\beta} & \Theta^Q_{\beta\xi} \\ \Theta^Q_{\xi\delta} & \Theta^Q_{\xi\beta} & \Theta^Q_{\xi\xi} \end{bmatrix}$$

where the size of the sub-matrices conforms to the size of the vectors $\boldsymbol{\delta_t}$, $\boldsymbol{\beta_t}$, and $\boldsymbol{\xi_t}$.

We begin with the recursion for bonds. The Nelson and Siegel parametrization implies that bond prices depend only on $\boldsymbol{\delta_t}$ (i.e. $B_\tau = -[\tau, \frac{1-e^{\zeta_1\tau}}{\zeta_1}, \frac{1-e^{\zeta_1\tau}}{\zeta_1} - \tau e^{-\zeta_1\tau}, \mathbf{0}_{1\times 6}]'$). Therefore, the non-zero elements of (A.3) satisfy

$$\begin{bmatrix} -\tau \\ -\frac{1-e^{\zeta_1\tau}}{\zeta_1} \\ \frac{1-e^{\zeta_1\tau}}{\zeta_1} - \tau e^{-\zeta_1\tau} \end{bmatrix} = \Theta^{Q\prime}_{\delta\delta} \begin{bmatrix} -(\tau-1) \\ -\frac{1-e^{\zeta_1(\tau-1)}}{\zeta_1} \\ \frac{1-e^{\zeta_1(\tau-1)}}{\zeta_1} - (\tau-1)e^{-\zeta_1(\tau-1)} \end{bmatrix} - \begin{bmatrix} 1 \\ -\frac{1-e^{\zeta_1}}{\zeta_1} \\ \frac{1-e^{\zeta_1}}{\zeta_1} - e^{-\zeta_1} \end{bmatrix}$$

which, in turn, implies

$$\Theta^{Q}_{\delta\delta} = \begin{bmatrix} 1 & 0 & 0 \\ 0 & e^{-\zeta_1} & \zeta_1 e^{-\zeta_1} \\ 0 & 0 & e^{-\zeta_1} \end{bmatrix}.$$

This condition for the arbitrage-free Nelson-Siegel model in discrete time was obtained by Hong, Niu, and Zeng (2016).[18]

Consider the parameters associated with the commodity factors. The Nelson-Siegel parametrization implies that the first three elements of $H^{\tilde{m}}_{\tau}$ are zero. Thus, (A.4) imposes

$$\begin{bmatrix} 1 \\ \tau \\ \frac{1-e^{\zeta_2\tau}}{\zeta_2} \\ \frac{1-e^{\zeta_2\tau}}{\zeta_2} - \tau e^{-\zeta_2\tau} \\ e^{-\omega\tau}\cos(\frac{2\pi}{12}(\tilde{m}+\tau)) \\ e^{-\omega\tau}\sin(\frac{2\pi}{12}(\tilde{m}+\tau)) \end{bmatrix} = \begin{bmatrix} \Theta^{Q}_{\beta\beta} & \Theta^{Q}_{\beta\xi} \\ \Theta^{Q}_{\xi\beta} & \Theta^{Q}_{\xi\xi} \end{bmatrix}' \begin{bmatrix} 1 \\ \tau-1 \\ \frac{1-e^{\zeta_2(\tau-1)}}{\zeta_2} \\ \frac{1-e^{\zeta_2(\tau-1)}}{\zeta_2} - (\tau-1)e^{-\zeta_2(\tau-1)} \\ e^{-\omega(\tau-1)}\cos(\frac{2\pi}{12}(\tilde{m}+1+\tau-1)) \\ e^{-\omega(\tau-1)}\sin(\frac{2\pi}{12}(\tilde{m}+1+\tau-1)) \end{bmatrix} \tag{A.5}$$

and

$$\begin{bmatrix} 1 \\ \frac{1-e^{\zeta_1\tau}}{\zeta_1} \\ \frac{1-e^{\zeta_1\tau}}{\zeta_1} - \tau e^{-\zeta_1\tau} \end{bmatrix} = \begin{bmatrix} \Theta^{Q\prime}_{\beta\delta} & \Theta^{Q\prime}_{\xi\delta} \end{bmatrix} \begin{bmatrix} 1 \\ \tau-1 \\ \frac{1-e^{\zeta_2(\tau-1)}}{\zeta_2} \\ \frac{1-e^{\zeta_2(\tau-1)}}{\zeta_2} - (\tau-1)e^{-\zeta_2(\tau-1)} \\ e^{-\omega(\tau-1)}\cos(\frac{2\pi}{12}(\tilde{m}+1+\tau-1)) \\ e^{-\omega(\tau-1)}\sin(\frac{2\pi}{12}(\tilde{m}+1+\tau-1)) \end{bmatrix}. \tag{A.6}$$

It is easy to verify that (A.5) implies $\Theta^{Q}_{\xi\beta} = \mathbf{0}_{2\times4}$, $\Theta^{Q}_{\beta\xi} = \mathbf{0}_{4\times2}$,

$$\Theta^{Q}_{\xi\xi} = \begin{bmatrix} e^{-\omega} & 0 \\ 0 & e^{-\omega} \end{bmatrix} \quad \text{and} \quad \Theta^{Q}_{\beta\beta} = \begin{bmatrix} 1 & 1 & \frac{1-e^{-\zeta_2}}{\zeta_2} & \frac{1-e^{-\zeta_2}}{\zeta_2} - e^{-\zeta_2} \\ 0 & 1 & 0 & 0 \\ 0 & 0 & e^{-\zeta_2} & \zeta_2 e^{-\zeta_2} \\ 0 & 0 & 0 & e^{-\zeta_2} \end{bmatrix}$$

[18] Joslin, Singleton, and Zhu (2011) show that the arbitrage-free Nelson-Siegel model imposes a single restriction on their maximally flexible (identified) model. In particular, the unconstrained case replaces the 1 in the $\Theta^{Q}_{\delta\delta}$ matrix by a free parameter.

while (A.6) implies $\Theta^{Q}_{\xi\delta} = \mathbf{0}_{2\times 3}$ and

$$\Theta^{Q}_{\beta\delta} = \begin{bmatrix} 1 & \frac{1-e^{-\zeta_1}}{\zeta_1} & \frac{1-e^{-\zeta_1}}{\zeta_1} - e^{-\zeta_1} \\ 0 & 0 & 0 \\ 0 & 0 & 0 \end{bmatrix}.$$

Lastly, (A.3), (A.4), and $D^{\tilde{m}}_{\tau} = H^{\tilde{m}}_{\tau} - B_{\tau}$ imply $\Theta^{Q}_{\delta\beta} = \mathbf{0}_{3\times 4}$ and $\Theta^{Q}_{\delta\xi} = \mathbf{0}_{3\times 2}$.□

B Appendix: Risk premia

The (realized) 1-period holding return of a τ-month contract is

$$f^{\tau-1}_{t+1} - f^{\tau}_{t} = C^{m_{t+1}}_{\tau-1} + D^{m_{t+1}\prime}_{\tau-1} X_{t+1} - C^{m_t}_{\tau} - D^{m_t\prime}_{\tau} X_t.$$

Using (5), (9), (10), (15), and (16) the time-t expected 1-period holding return can be written as

$$E_t[f^{\tau-1}_{t+1} - f^{\tau}_{t}] = \frac{1}{2}[B'_{\tau-1}\Gamma\Gamma'B_{\tau-1} - H^{m_{t+1}\prime}_{\tau-1}\Gamma\Gamma'H^{m_{t+1}}_{\tau-1}] + D^{m_{t+1}\prime}_{\tau-1}\Gamma\Lambda_t.$$

The spot premium is the 1-period holding return of a futures contract with settlement date in the next month. Using $f^{0}_{t+1} = s_{t+1}$, $B_0 = 0$ and $H^{m_{t+1}}_{0} = D^{m_{t+1}}_{0} = \gamma^{m_{t+1}}_{1}$, the spot premium is

$$E_t[s_{t+1} - f^{1}_{t}] = -\frac{1}{2}[\gamma^{m_{t+1}\prime}_{1}\Gamma\Gamma'\gamma^{m_{t+1}}_{1}] + \gamma^{m_{t+1}\prime}_{1}\Gamma\Lambda_t.$$

The term premium and the h-period holding returns follow from simple manipulations of the 1-period holding returns and the spot premium, as described in the text.

Table 1: **Test of stochastic versus deterministic seasonality in futures prices**

The table shows tests of deterministic versus stochastic seasonality in heating oil futures. τ stands for maturity. CH denotes Canova and Hansen (1995) test, while BH denotes Busetti and Harvey (2003) parametric and nonparametric tests. Under the null hypothesis of deterministic seasonality, the statistics are distributed as a generalized Von-Mises random variable with 2 degrees of freedom. ***/**/* denote significance at 1/5/10 percent level. For gasoil, data starts in August 1990; for Gasoline, in January 1985; for Natural Gas, in April 1990; for all other commodities, the sample starts on the last day of 1983. For all commodities the ending date is April 2017.

	Contract Maturity τ months					
Energy	1	2	3	6	9	12
Gasoil						
CH	3.7065***	1.0628**	0.9536**	0.6203*	0.3104	0.6865*
BH (nonparam.)	4.4755***	1.7076***	1.9084***	0.9575**	0.1455	0.5695
BH (param.)	11.738***	1.3052***	3.7776***	7.5316***	1.8639***	1.2931***
Gasoline						
CH	0.7967**	0.8284**	0.8368**	0.4411	0.8771**	2.2912***
BH (nonparam.)	1.155***	1.3338***	1.4022***	0.1824	0.2539	2.244***
BH (param.)	3.8417***	0.4951	1.7158***	26.415***	4.5124***	0.4165
Heating Oil						
CH	0.8418**	0.768**	0.6652*	0.1954	0.8524**	1.4317***
BH (nonparam.)	1.0308**	1.2491***	1.2211***	0.2055	0.9599**	1.5977***
BH (param.)	5.303***	11.162***	15.177***	9.5591***	1.0832***	15.704***
Natural Gas						
CH	1.542***	0.3236	0.2023	0.4106	0.8064**	0.2779
BH (nonparam.)	3.5174***	0.3736	0.283	0.7733**	0.4905	0.398
BH (param.)	4.2392***	14.496***	18.123***	1.2262***	13.781***	6.514***
Agricultural						
Corn						
CH	8.1784***	0.8555**	0.7226*	0.9563**	2.4234***	2.5611***
BH (nonparam.)	18.572***	1.2667***	0.3207	1.0738***	6.5478***	7.4085***
BH (param.)	1.3201***	7.0038***	1.6591***	6.8562***	8.2679***	8.3063***
Wheat						
CH	5.9498***	1.6014***	0.4361	1.0749***	1.0055**	0.2214
BH (nonparam.)	7.8489***	3.061***	0.3709	0.508	1.2175***	0.2855
BH (param.)	1.5193***	5.1433***	1.6911***	0.1694	1.3814***	4.6131***
Soybean						
CH	10.119***	0.4443	0.5835	1.1623***	2.8187***	4.9593***
BH (nonparam.)	0.9757**	0.7387*	0.4419	0.4659	7.8844***	11.549***
BH (param.)	4.3753***	6.7288***	2.0364***	7.0118***	9.9595***	12.379***

Table 2: **Number of factors in the yield curve and the cost-of-carry curve**

The table reports the contribution of the first three principal components to the variability of the yield curve and the cost-of-carry curve. $\epsilon_t^{(\tau),CS}$ refers to the cost-of-carry curve obtained from the cross-sectional regressions and $\epsilon_t^{(\tau),KF}$ is the cost-of-carry curve estimated using the Kalman filter.

	PC1	PC2	PC3
Yield Curve			
$y_t^{(\tau)}$	99.67	0.31	0.02
Energy			
Gasoil			
$\epsilon_t^{(\tau),CS}$	45.52	19.84	11.28
$\epsilon_t^{(\tau),KF}$	72.46	5.65	4.00
Gasoline			
$\epsilon_t^{(\tau),CS}$	35.24	28.08	13.61
$\epsilon_t^{(\tau),KF}$	38.59	19.62	11.98
Heating Oil			
$\epsilon_t^{(\tau),CS}$	50.59	20.10	12.04
$\epsilon_t^{(\tau),KF}$	63.61	16.42	5.58
Natural Gas			
$\epsilon_t^{(\tau),CS}$	80.55	7.96	5.15
$\epsilon_t^{(\tau),KF}$	55.92	16.57	14.03
Agricultural			
Corn			
$\epsilon_t^{(\tau),CS}$	25.31	16.60	12.41
$\epsilon_t^{(\tau),KF}$	28.22	18.28	12.26
Wheat			
$\epsilon_t^{(\tau),CS}$	22.59	17.22	14.37
$\epsilon_t^{(\tau),KF}$	35.48	19.59	10.79
Soybean			
$\epsilon_t^{(\tau),CS}$	16.07	14.10	13.25
$\epsilon_t^{(\tau),KF}$	26.83	17.14	11.76

Table 3: **Estimates of the model with stochastic seasonality**

Parameters of the VAR(1) process for the yield, the spot and cost-of-carry factors

$\mu_\delta\,(\times 1000)$

$$\begin{bmatrix} 0.1305 \\ (0.048) \\ 0.0064 \\ (0.0593) \\ 0.0255 \\ (0.1072) \end{bmatrix}$$

$\Theta_{\delta\delta}$

$$\begin{bmatrix} 0.964 & 0.006 & 0.026 \\ (0.012) & (0.019) & (0.011) \\ -0.005 & 0.945 & 0.031 \\ (0.014) & (0.021) & (0.014) \\ -0.004 & 0.016 & 0.936 \\ (0.023) & (0.028) & (0.016) \end{bmatrix}$$

$\Gamma_{\delta\delta}\,(\times 1000)$

$$\begin{bmatrix} 0.313 & 0 & 0 \\ (0.011) & & \\ -0.267 & 0.218 & 0 \\ (0.014) & (0.008) & \\ -0.167 & -0.027 & 0.646 \\ (0.021) & (0.026) & (0.022) \end{bmatrix}$$

$\mu_\beta\,(\times 100)$

$$\begin{bmatrix} -0.0134 \\ (0.9908) \\ -0.0654 \\ (0.0229) \\ -0.01864 \\ (0.4807) \\ 0.5343 \\ (0.3542) \end{bmatrix}$$

$\Theta_{\beta\beta}$

$$\begin{bmatrix} 0.9908 & 0.1691 & 0.8391 & -0.0085 \\ (0.012) & (1.045) & (0.199) & (0.242) \\ 0.0004 & 0.8876 & 0.0185 & 0.0238 \\ (0.0002) & (0.025) & (0.005) & (0.007) \\ 0.0002 & -0.8541 & 0.8254 & 0.5384 \\ (0.0044) & (0.555) & (0.072) & (0.102) \\ 0.0007 & 1.2311 & -0.2151 & 0.3386 \\ (0.0028) & (0.428) & (0.067) & (0.091) \end{bmatrix}$$

$\Gamma_{\beta\beta}\,(\times 100)$

$$\begin{bmatrix} 9.634 & 0 & 0 & 0 \\ (0.04) & & & \\ -0.141 & 0.139 & 0 & 0 \\ (0.012) & (0.009) & & \\ -0.971 & -0.004 & 2.915 & 0 \\ (0.197) & (0.309) & (0.323) & \\ -0.143 & -0.488 & -2.006 & 1.138 \\ (0.175) & (0.287) & (0.255) & (0.069) \end{bmatrix}$$

Volatility of seasonal process

$\sigma_\xi = 0.0029\,(0.0002)$ $\quad \sigma_{\xi^*} = 0.0017\,(0.0001)$

Other parameters and log-likelihood

$\zeta_1 = 0.053\,(0.0006)$ $\quad \zeta_2 = 0.416\,(0.021)$ $\quad \omega = 0.0096\,(0.0014)$ $\quad$ Log-likelihood = 51270.95

Table 4: **Pricing errors**

The table compares the pricing errors in the models with stochastic (SS) and deterministic (DS) seasonality. RMSPE is the root mean square pricing error and MAPE is the mean absolute pricing error. All entries are multiplied by 100.

	RMSPE		MAPE	
Maturity	SS	DS	SS	DS
1	0.673	1.996	6.847	12.659
3	0.210	0.593	3.905	6.760
6	0.416	0.582	5.696	6.759
9	0.431	0.648	5.750	7.229
12	0.364	0.691	5.171	7.446
16	0.245	0.825	4.391	8.183

Figure 1: **Spot, cost-of-carry, and seasonal factors**

Estimates of commodity factors of the models with stochastic and deterministic seasonality: deseasonalized spot β_{0t}; factors of the cost-of-carry, β_{1t}, β_{2t}, and $\beta 3_{3t}$; and seasonal factors ξ_t and ξ_t^*.

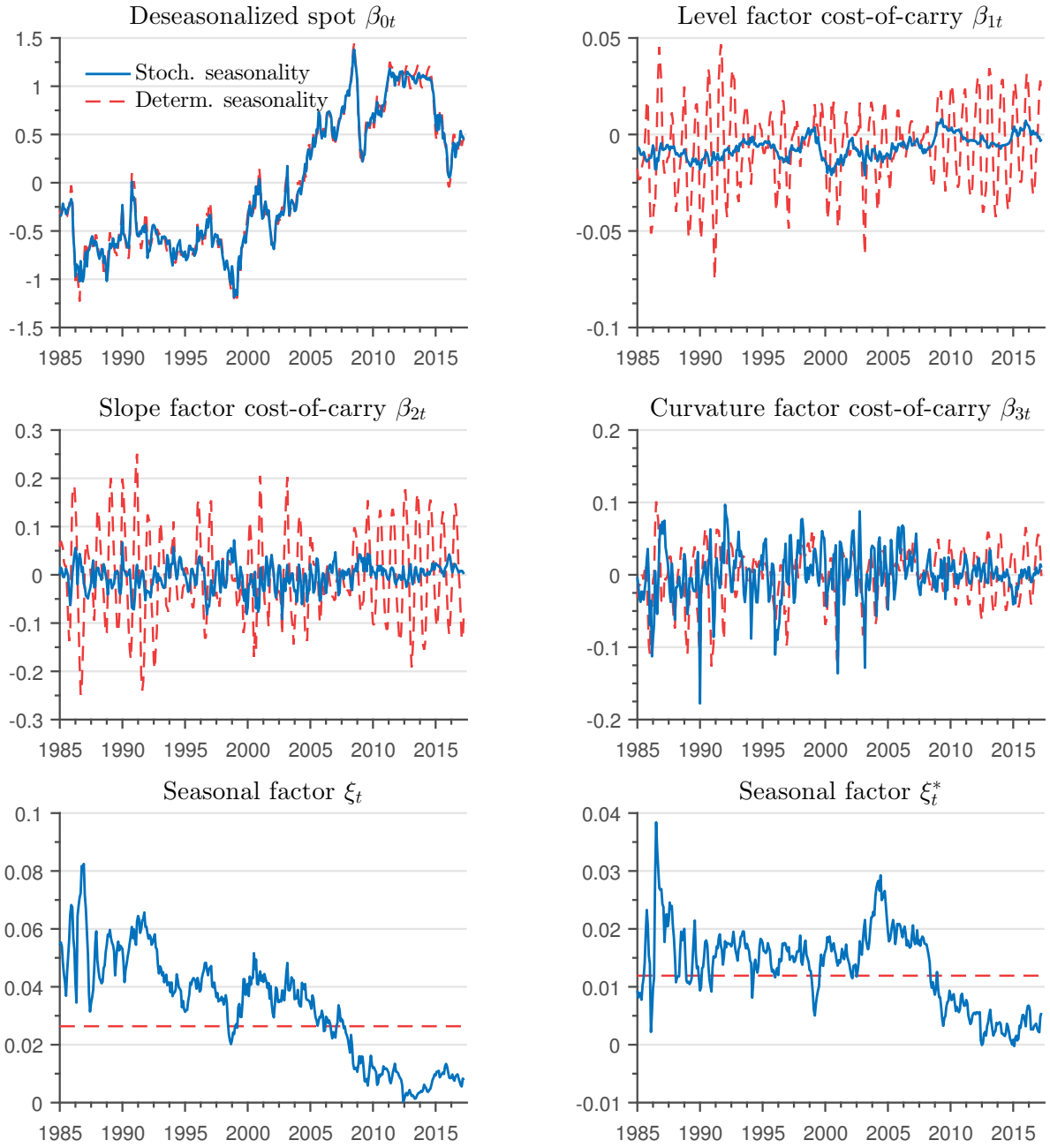

Figure 2: Seasonal component and heating oil inventories

The upper panel displays the implied seasonal component $\xi_t \cos(\frac{2\pi}{12} m_t) + \xi_t^* \sin(\frac{2\pi}{12} m_t)$ in the models with stochastic and deterministic seasonality. The figure also displays the months in circles in the model with stochastic seasonality. Most seasonal peaks are in December (D) and troughs in June (J). The bottom left panel displays the seasonal component of log-inventories and the implied seasonal component of the spot commodity price, both standardized. The bottom right panel shows the cost-of-carry level factor β_{1t} and the non-seasonal component of log-inventories, both standardized.

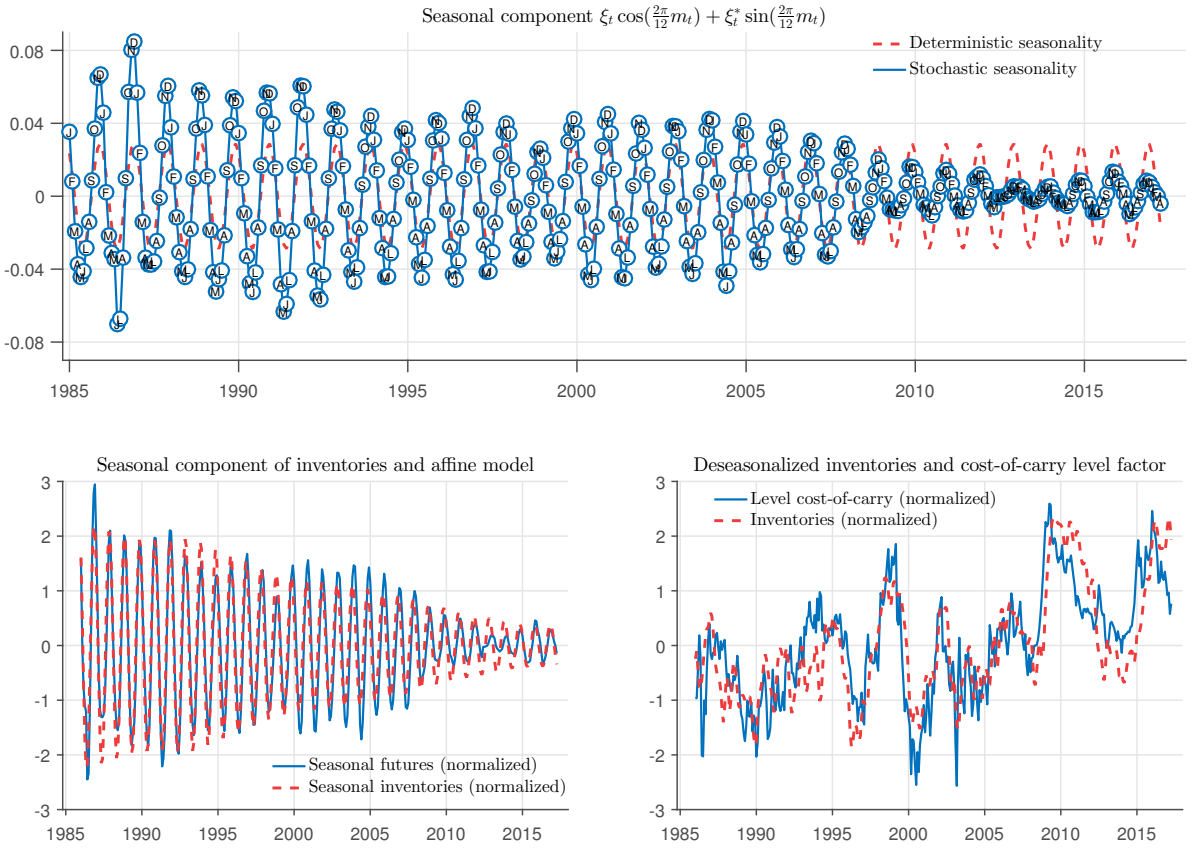

Figure 3: Fitted log-futures curves

The figure shows fitted log-futures curves, deseasonalized fitted log-futures curve, and actual log-futures prices on selected dates.

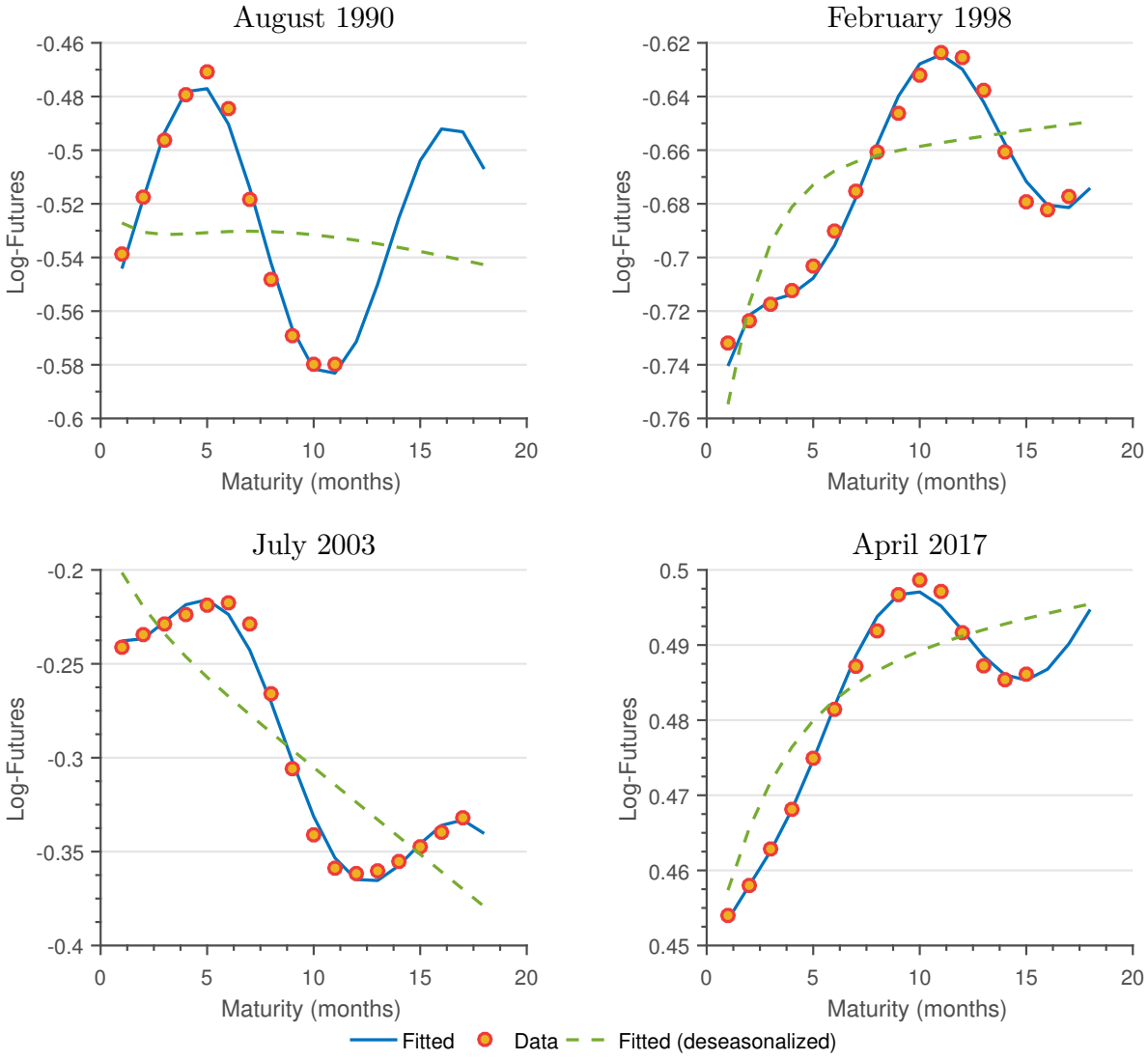

Figure 4: Expected 1-month holding futures returns

This figures shows the expected 1-month holding returns of a 1-month and a 18-months futures contract. Returns are expressed in percentage points and on an annualized basis. The upper left panel displays the total expected return. The other panels display the contribution of the different factors. The upper right panel also shows the negative of the level factor of the interest rates and the bottom left panel adds the level of the cost-of-carry factor.

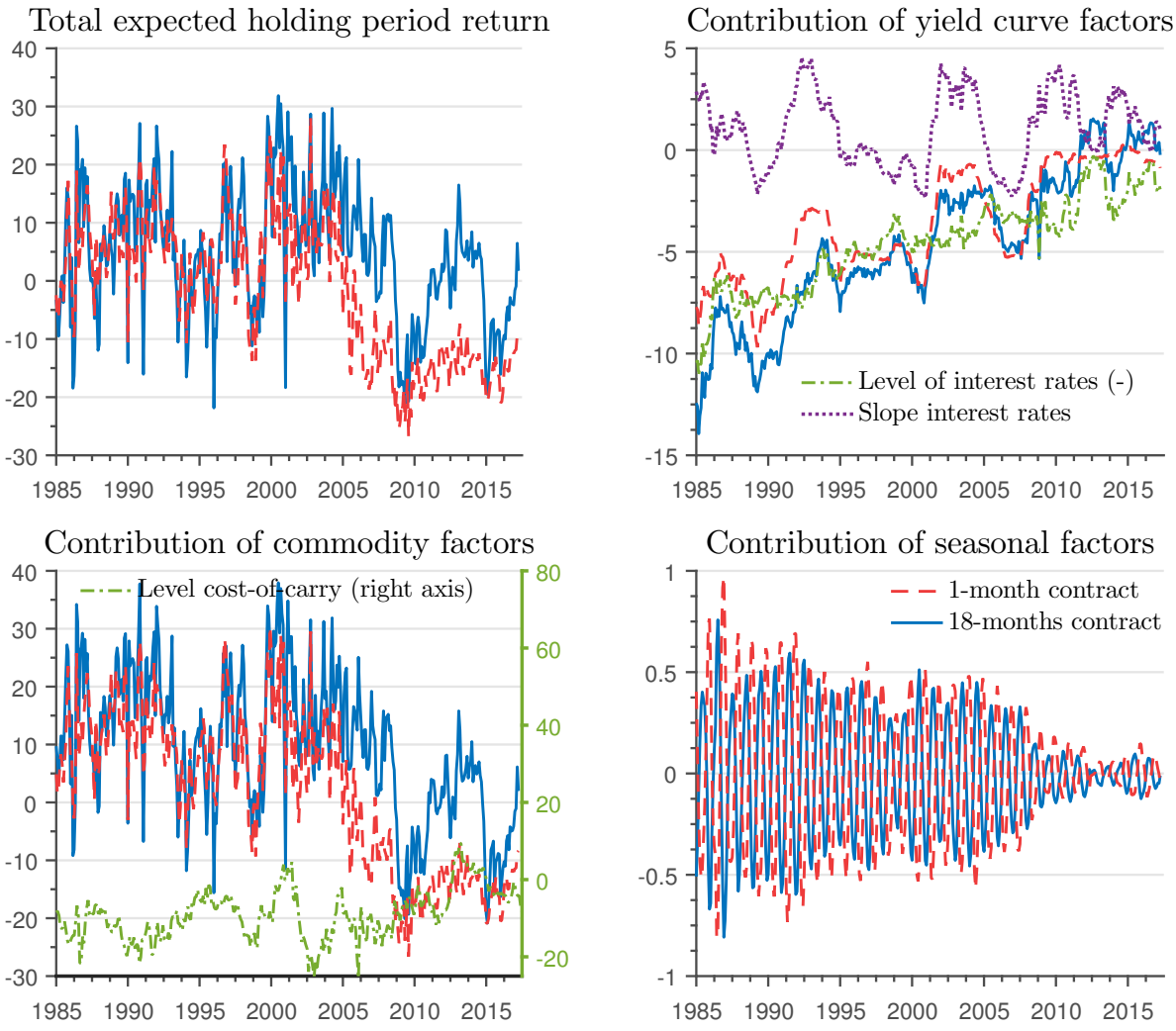

Figure 5: Expected holding futures returns of an 18-month futures contract

Expected 1-month and 18-months holding returns of an 18-months futures contract. Returns are expressed in percentage points and on an annualized basis. The upper left panel displays the total expected return. The other panels display the contribution of the different factors. The upper right panel also shows the negative of the level factor and the slope of the interest rates and the bottom left panel adds the commodity spot factor.

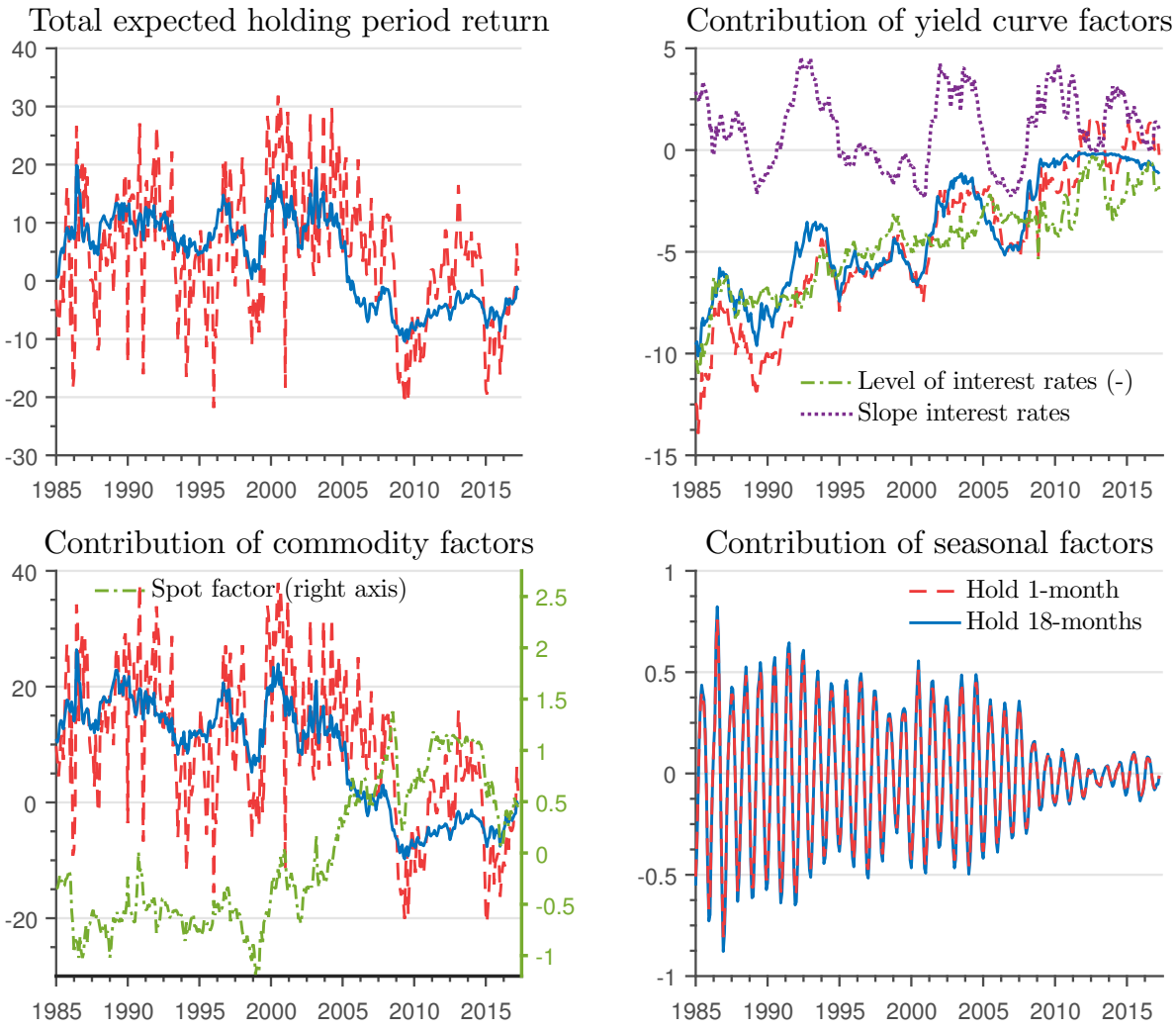

Figure 6: Comparing models with and without imposing the zero lower bound on interest rates

The figure compares some results for the baseline model (solid lines) with those estimated imposing the zero lower bound (dashed lines) on interest rates (ZLB).

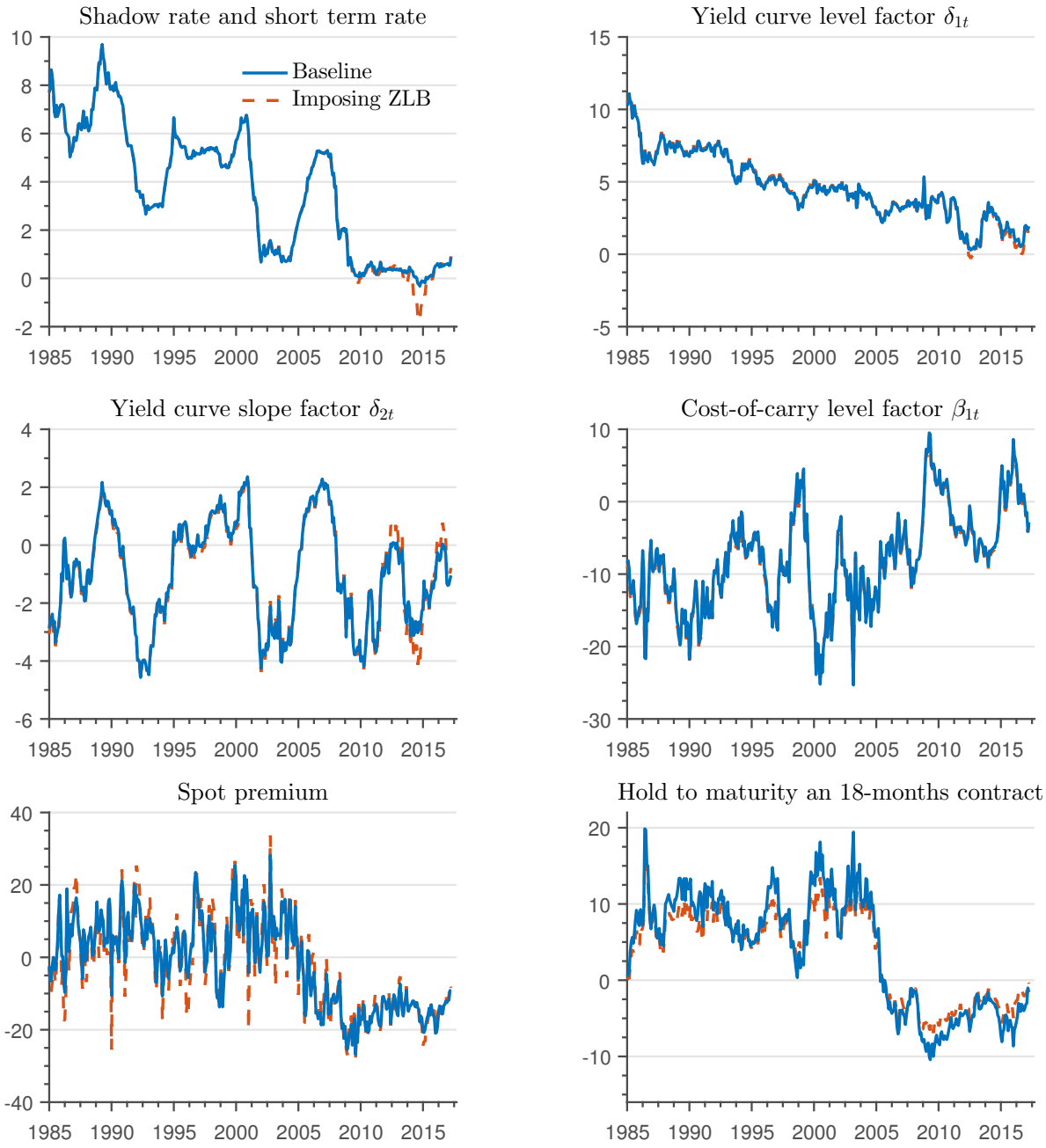

Figure 7: Spot and term premium: a case study

The upper left panel displays the spot price (solid line) and all futures prices (dotted lines). The upper right panel displays the spot and term premium during the peak and trough months of heating oil prices. The bottom panels display the fitted and actual futures curves on the same dates.

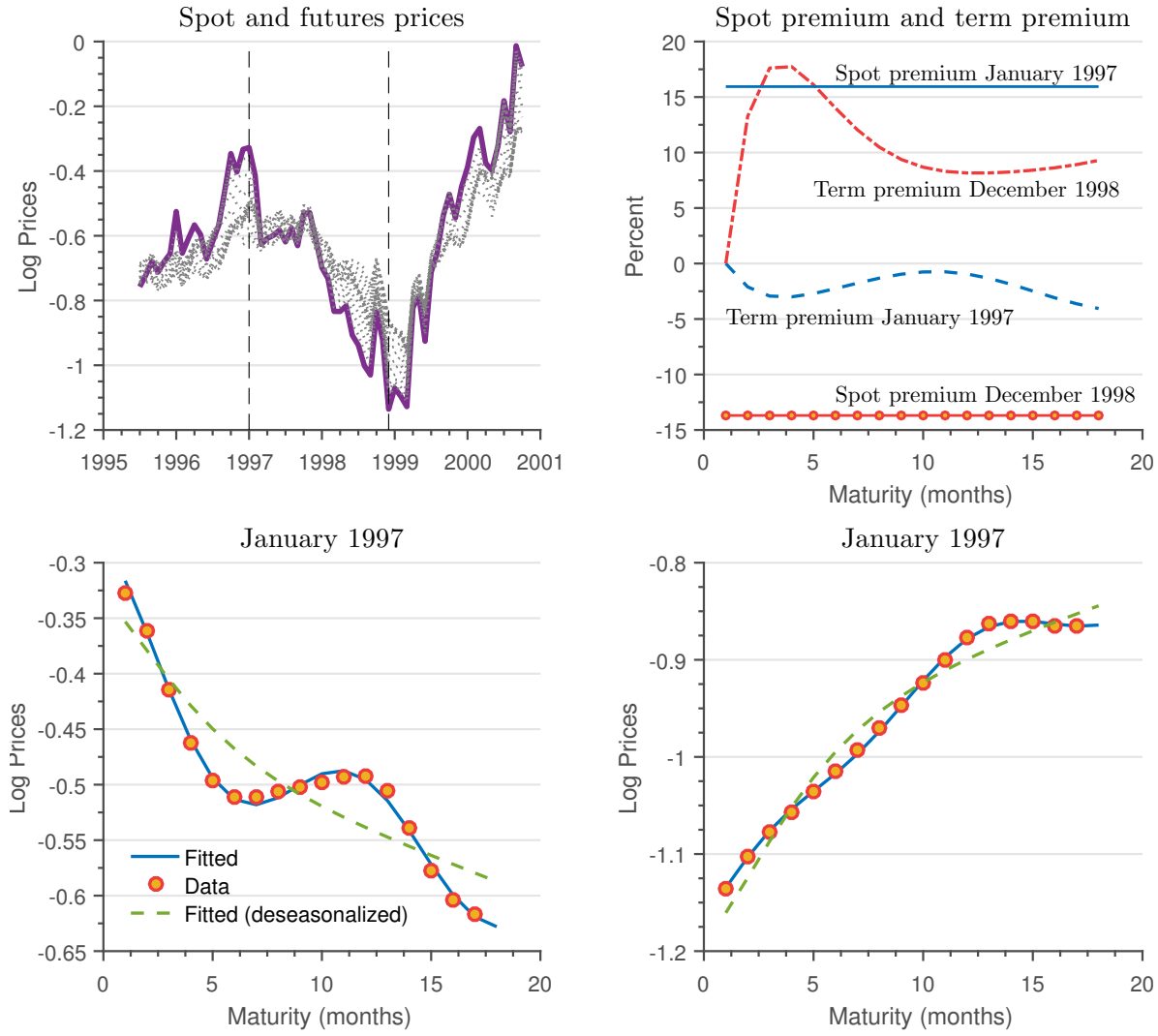

Supplement to "Risk Premia and Seasonality in Commodity Futures"

Constantino Hevia
Universidad Torcuato Di Tella

Ivan Petrella
Warwick Business School

Martin Sola
Universidad Torcuato Di Tella

March 5, 2018

Contents

A Appendix: Data description

We use data on U.S. zero coupon bonds and commodities futures for the period Jan-1984 through Apr-2017. We use data on commodity futures prices published by the relevant exchanges, and freely available from the web provider www.quandl.com. We gather data on four energy commodities (gasoil, gasoline, heating oil, and natural gas) and three agricultural commodities (corn, soybean, and wheat). Those commodities account for more than 40% of the weight in the main commodity indexes.[1] We use end-of-month log settlement prices and consider contracts with maturities up to 18 months. Available maturities have varied over time. For example, in the early part of our sample heating oil contracts were available with maturities up to 12 months. Contracts with maturities up to 18 months in the future appeared in 1991. For agricultural commodities delivery occurs on certain months of the year. There are five delivery months for corn and wheat, and seven for soybean.

To reduce the problem of low contract liquidity, we do not use data for contracts in the expiration month and contracts with a zero monthly return. We drop from our sample the contracts closest to expiration and label a 1 month futures contract those that expire in the month after the next month and likewise for the longer maturities. We impose this convention for two reasons. First, delivery for contracts that are about to expire can be made as early as six days after the last trading day. Second, futures contracts become very illiquid a couple of weeks before expiration. We also exclude contracts for which there are less than 100 trades within the month. This filter leads to the exclusion of 3 to 5 percent of the data depending on the commodity.

For bond yields, we use Gürkaynak et al. (2007) estimate of the yield curve for maturities of 3, 6, 12, 24, 36, 48, and 60 months. The dates are matched with those of the commodities futures. To evaluate the model, we also use data on inventories (U.S. Ending Stock of

[1] Crude oil (WTI and Brent) typically accounts for more than 30% of the index. The rest is divided among metals, soft commodities, and livestock.

Distillate Fuel Oil) obtained from the U.S. Energy Information Administration.

B Proof of Proposition 1: Cost-of-carry process

We guess-and-verify that $c_t = \psi_0^{m_t} + \psi_1^{m_t\prime} X_t$ for some values $\psi_0^{m_t}$ and $\psi_1^{m_t}$. Take an arbitrary month $m_t = \tilde{m}$. Using the guess and equations (5), (6), (12) into the pricing condition (13) gives

$$\begin{aligned}\exp(\gamma_0 + \gamma_1^{\tilde{m}\prime}) = &\exp\left(-\rho_0 - \rho_1' X_t + \gamma_0 - \psi_0^{\tilde{m}+1} + \left(\gamma_1^{\tilde{m}+1} - \psi_1^{\tilde{m}+1}\right)'(\mu + \Theta X_t) - \tfrac{1}{2}\Lambda_t'\Lambda_t\right) \\ &\times E_t\left[\exp\left(\left[(\gamma_1^{\tilde{m}+1} - \psi_1^{\tilde{m}+1})'\Gamma - \Lambda_t\right]\eta_{t+1}\right)\right].\end{aligned}$$

Solving the expectation,

$$\begin{aligned}&E_t\left[\exp\left(\left[(\gamma_1^{\tilde{m}+1} - \psi_1^{\tilde{m}+1})'\Gamma - \Lambda_t\right]\eta_{t+1}\right)\right] \\ &= \exp\left((\gamma_1^{\tilde{m}+1} - \psi_1^{\tilde{m}+1})'\tfrac{\Gamma'\Gamma}{2}(\gamma_1^{\tilde{m}+1} - \psi_1^{\tilde{m}+1}) - (\gamma_1^{\tilde{m}+1} - \psi_1^{\tilde{m}+1})'\Gamma\Lambda_t + \tfrac{1}{2}\Lambda'\Lambda_t\right)\end{aligned}$$

Replacing this expression above, using $\Lambda_t = \lambda_0 + \lambda_1 X_t$, and rearranging gives

$$\begin{aligned}\gamma_1^{\tilde{m}\prime} X_t = &-\rho_0 - \psi_0^{\tilde{m}+1} + (\gamma_1^{\tilde{m}+1} - \psi_1^{\tilde{m}+1})'(\mu - \Gamma\lambda_0) \\ &+ (\gamma_1^{\tilde{m}+1} - \psi_1^{\tilde{m}+1})'\tfrac{\Gamma'\Gamma}{2}(\gamma_1^{\tilde{m}+1} - \psi_1^{\tilde{m}+1}) + \left[(\gamma_1^{\tilde{m}+1} - \psi_1^{\tilde{m}+1})'(\Theta - \Gamma\lambda_1) - \rho_1'\right] X_t.\end{aligned}$$

Matching coefficients gives the values of $\psi_0^{\tilde{m}+1}$ and $\psi_1^{\tilde{m}+1}$ displayed in Proposition 1.□

C Further empirical properties of commodity futures

Table 1 and Table 2 show tests of specification of the stochastic seasonal pattern for heating oil and soybeans. In both cases, the data supports a specification of stochastic seasonality with a single pair of seasonal factors, associated with the fundamental frequency.

Table 1: **Heating oil. Number of seasonal factors**

The stochastic seasonal component is driven by pairs of seasonal factors $z_t^s = \sum_{j=1}^{6}[\xi_{jt}\cos(\frac{2\pi j}{12}m_t) + \xi_{jt}^*\sin(\frac{2\pi j}{12}m_t)]$. We test restricted versions of the seasonality process of the form $z_t^s = \sum_{j=1}^{J}[\xi_{jt}\cos(\frac{2\pi j}{12}m_t) + \xi_{jt}^*\sin(\frac{2\pi j}{12}m_t)]$, where $J = 1, 2, .., 6$ indicates the number of seasonal factors (i.e. harmonics) included in the specification. Each column of the table corresponds to a different specification of the seasonal component and τ stands for maturity of the contract. For each specification we report the log likelihood value, the Akaike (AIC) and Bayesian (BIC) information criteria. Bold numbers denote the minimum values of the information criteria.

	$J = 1, \sigma_1^2 \neq \sigma_1^{*2}$	$J = 1, \sigma_1^2 = \sigma_1^{*2}$	$J = 2, \sigma_j^2 = \sigma_j^{*2}$	$J = 6, \sigma_j^2 = \sigma_j^{*2}$
1-month futures $(\tau = 1)$				
LogLik	-1136.444	-1136.546	-1143.820	-1177.912
AIC	**2288.888**	2289.092	2307.641	2397.824
BIC	**2320.820**	2321.024	2347.555	2481.645
2-month futures $(\tau = 2)$				
LogLik	-1112.152	-1112.232	-1116.865	-1152.498
AIC	**2240.305**	2240.465	2253.730	2346.996
BIC	**2272.237**	2272.396	2293.645	2430.817
3-month futures $(\tau = 3)$				
LogLik	-1094.235	-1094.443	-1096.279	-1132.514
AIC	**2204.470**	2204.887	2212.558	2307.029
BIC	**2236.402**	2236.818	2252.472	2390.850
6-month futures $(\tau = 6)$				
LogLik	-1025.031	-1025.134	-1033.368	-1070.923
AIC	**2066.062**	2066.269	2086.737	2183.847
BIC	**2097.994**	2098.201	2126.652	2267.667
9-month futures $(\tau = 9)$				
LogLik	-917.410	-917.524	-920.994	-960.407
AIC	**1850.820**	1851.048	1861.988	1962.814
BIC	**1882.752**	1882.979	1901.902	2046.635
12-month futures $(\tau = 12)$				
LogLik	-768.907	-769.729	-778.106	-818.339
AIC	**1553.814**	1555.458	1576.212	1678.679
BIC	**1585.746**	1587.389	1616.126	1762.500

Table 2: **Soybean. Number of seasonal factors**

The stochastic seasonal component is driven by pairs of seasonal factors $z_t^s = \sum_{j=1}^{6}[\xi_{jt}\cos(\frac{2\pi j}{12}m_t) + \xi_{jt}^*\sin(\frac{2\pi j}{12}m_t)]$. We test restricted versions of the seasonality process of the form $z_t^s = \sum_{j=1}^{J}[\xi_{jt}\cos(\frac{2\pi j}{12}m_t) + \xi_{jt}^*\sin(\frac{2\pi j}{12}m_t)]$, where $J = 1, 2, .., 6$ indicates the number of seasonal factors (i.e. harmonics) included in the specification. Each column of the table corresponds to a different specification of the seasonal component and τ stands for maturity of the contract. For each specification we report the log likelihood value, the Akaike (AIC) and Bayesian (BIC) information criteria. Bold numbers denote the minimum values of the information criteria.

	$J = 1, \sigma_1^2 \neq \sigma_1^{*2}$	$J = 1, \sigma_1^2 = \sigma_1^{*2}$	$J = 2, \sigma_j^2 = \sigma_j^{*2}$	$J = 6, \sigma_j^2 = \sigma_j^{*2}$
1-month futures $(\tau = 1)$				
LogLik	-694.330	-694.611	-697.740	-701.091
AIC	**1404.660**	1405.222	1415.479	1444.182
BIC	**1436.591**	1437.153	1455.394	1528.002
2-month futures $(\tau = 2)$				
LogLik	-689.491	-689.491	-698.668	-702.782
AIC	1394.982	**1394.982**	1417.336	1447.564
BIC	1426.914	**1426.914**	1457.251	1531.385
3-month futures $(\tau = 3)$				
LogLik	-668.562	-668.562	-676.283	-680.497
AIC	1353.124	**1353.124**	1372.567	1402.994
BIC	1385.056	**1385.056**	1412.481	1486.815
6-month futures $(\tau = 6)$				
LogLik	-644.586	-644.586	-652.823	-656.847
AIC	1305.171	**1305.171**	1325.645	1355.694
BIC	1337.103	**1337.103**	1365.560	1439.514
9-month futures $(\tau = 9)$				
LogLik	-612.616	-612.616	-622.010	-626.675
AIC	1241.232	**1241.232**	1264.019	1295.351
BIC	1273.164	**1273.164**	1303.934	1379.171
12-month futures $(\tau = 12)$				
LogLik	-562.525	-562.820	-570.457	-574.430
AIC	**1141.050**	1141.639	1160.913	1190.860
BIC	**1172.981**	1173.571	1200.828	1274.681

Figure 1 show estimated seasonal factors extracted using an univariate model for each contract maturity in isolation. Clearly, the estimated seasonal factors depend on the particular maturity used to estimate the model. In other words, extracting the seasonal component from each futures contract in isolation does not generate a seasonal pattern consistent across maturities.

Figure 1: Estimated seasonality in commodity futures

The figure shows the estimated seasonal component using univariate models for each contract maturity in isolation. The estimated seasonal patterns are not consistent across contract maturities.

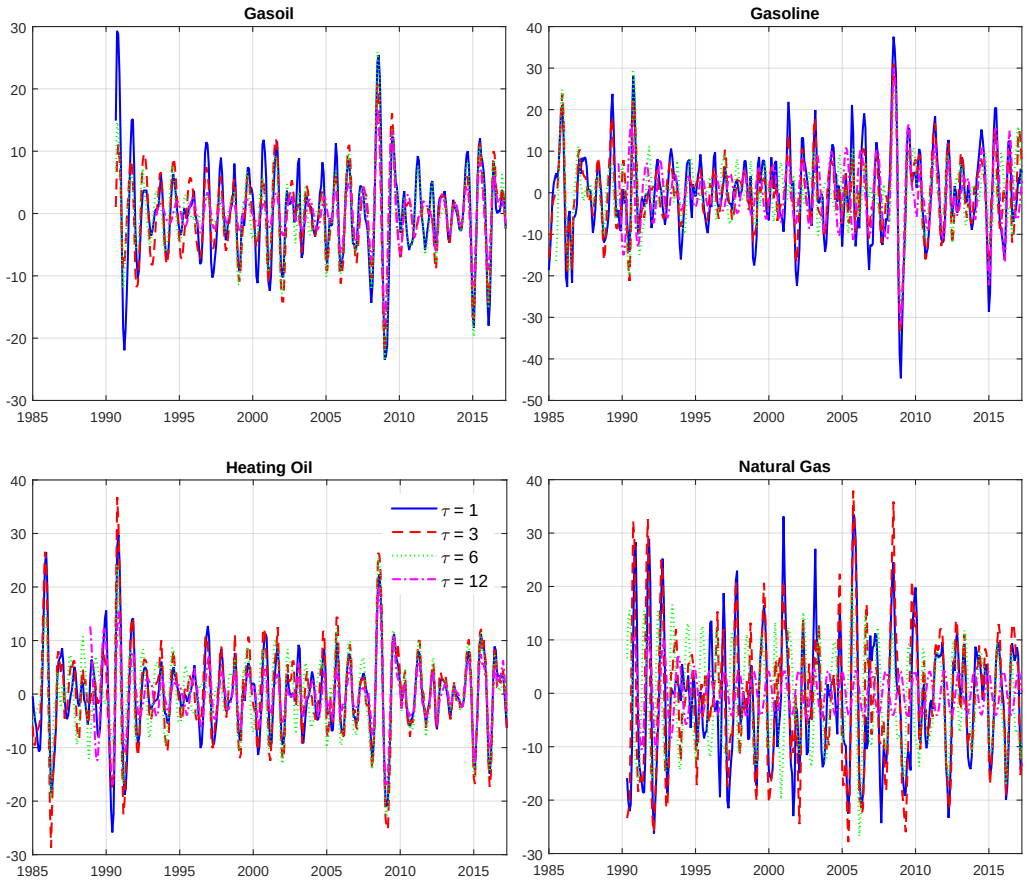

D Model with deterministic seasonality

Table 3 reports the estimates of the affine model of futures prices imposing deterministic seasonality using data on heating oil futures prices from January 1984 to April 2017.

Table 3: **Estimates of the model with deterministic seasonality**
The table shows the estimates of the model using futures prices on heating oil and imposing deterministic seasonality. The sample period is from January 1984 to April 2017.

Parameters of the VAR(1) process for the yield, the spot and cost-of-carry factors

$\mu_\delta\,(\times 1000)$

0.063
(0.048)
−0.0252
(0.0540)
−0.0503
(0.1095)

$\Theta_{\delta\delta}$

0.981	0.001	0.020
(0.012)	(0.018)	(0.010)
−0.0001	0.964	0.019
(0.013)	(0.020)	(0.014)
0.014	0.029	0.925
(0.024)	(0.025)	(0.026)

$\Gamma_{\delta\delta}\,(\times 1000)$

0.299	0	0
(0.009)		
−0.252	0.214	0
(0.013)	(0.007)	
−0.142	−0.033	0.627
(0.025)	(0.036)	(0.020)

$\mu_\beta\,(\times 100)$

0.753
(0.769)
−0.369
(0.071)
0.104
(0.135)
1.075
(0.289)

$\Theta_{\beta\beta}$

0.983	1.483	−0.004	−0.115
(0.010)	(0.817)	(0.197)	(0.208)
0.001	0.389	0.246	−0.065
(0.0007)	(0.065)	(0.019)	(0.022)
0.0005	0.078	1.149	0.230
(0.0015)	(0.141)	(0.037)	(0.032)
−0.001	1.855	−1.122	0.950
(0.0027)	(0.264)	(0.070)	(0.083)

$\Gamma_{\beta\beta}\,(\times 100)$

9.547	0	0	0
(0.039)			
−0.108	−0.623	0	0
(0.044)	(0.055)		
−0.691	−0.372	1.225	0
(0.091)	(0.132)	(0.083)	
0.131	2.488	−1.029	0.658
(0.205)	(0.230)	(0.099)	(0.031)

Parameters of seasonal process

$\xi_0 = 0.0263\,(0.0013)$ $\quad \xi_0^* = 0.0119\,(0.0014)$

Other parameters and log-likelihood

$\zeta_1 = 0.053\,(0.0006)$ $\quad \zeta_2 = 0.1967\,(0.00557)$ $\quad \omega = 0.0065\,(0.0062)$ $\quad$ Log-likelihood = 49004.145

E Estimation using data on soybean futures

In this section we show the estimation of the model using data on soybean futures. The sample period is from January 1984 to October 2016. Table 4 displays the estimates of the model with deterministic seasonality. Figure 2 displays the estimated commodity factors while Figure 3 shows actual and fitted log-futures curves on selected dates, including the estimates of the deseasonalized futures curve. Finally, Figure 4 shows the 1-month expected holding return for futures contracts that mature in 1 month and 18 months ahead while Figure 5 displays the expected risk premia of holding a 18 months futures contracts during 1 and 18 months. The interpretation of these plots is analogous to that discussed in the paper for the case of heating oil.

Table 4: **Soybean: Estimates of the model with stochastic seasonality**

The table shows the estimates of the baseline model using futures prices on soybean. The sample period is from January 1984 to October 2016.

Parameters of the VAR(1) process for the yield, the spot and cost-of-carry factors

$\mu_\delta\,(\times 1000)$

0.118
(0.054)
−0.0015
(0.0655)
−0.1327
(0.118)

$\Theta_{\delta\delta}$

0.967	−0.002	0.027
(0.012)	(0.021)	(0.012)
−0.007	0.947	0.022
(0.013)	(0.021)	(0.015)
0.0396	0.068	0.898
(0.024)	(0.032)	(0.026)

$\Gamma_{\delta\delta}\,(\times 1000)$

0.315	0	0
(0.011)		
−0.268	0.218	0
(0.015)	(0.008)	
−0.179	−0.030	0.633
(0.034)	(0.035)	(0.022)

$\mu_\beta\,(\times 100)$

−0.0131
(4.62)
−0.0815
(0.344)
−0.665
(8.79)
0.786
(6.11)

$\Theta_{\beta\beta}$

1.000	−0.028	0.635	0.015
(0.007)	(1.068)	(0.151)	(0.213)
0.000	0.927	0.008	−0.01
(0.0005)	(0.040)	(0.005)	(0.009)
−0.001	−1.351	0.786	0.654
(0.0133)	(0.851)	(0.148)	(0.171)
0.000	1.303	−0.220	0.437
(0.0092)	(0.529)	(0.106)	(0.114)

$\Gamma_{\beta\beta}\,(\times 100)$

7.0916	0	0	0
(0.042)			
−0.197	0.159	0	0
(0.021)	(0.022)		
0.145	−0.023	3.986	0
(0.178)	(0.152)	(0.757)	
0.001	−0.212	−3.248	0.731
(0.19)	(0.312)	(0.536)	(0.222)

Volatility of seasonal process

$\sigma_\xi = 0.0064\,(0.0007)$ $\quad \sigma_{\xi^*} = 0.0003\,(0.0002)$

Other parameters and log-likelihood

$\zeta_1 = 0.053\,(0.0007)$ $\quad \zeta_2 = 0.5435\,(0.0386)$ $\quad \omega = 0.0195\,(0.0059)$ $\quad$ Log-likelihood = 37948.583

Figure 2: **Soybean: Spot, cost-of-carry, and seasonal factors**

Estimates of commodity factors of the baseline model using data on soybean futures.

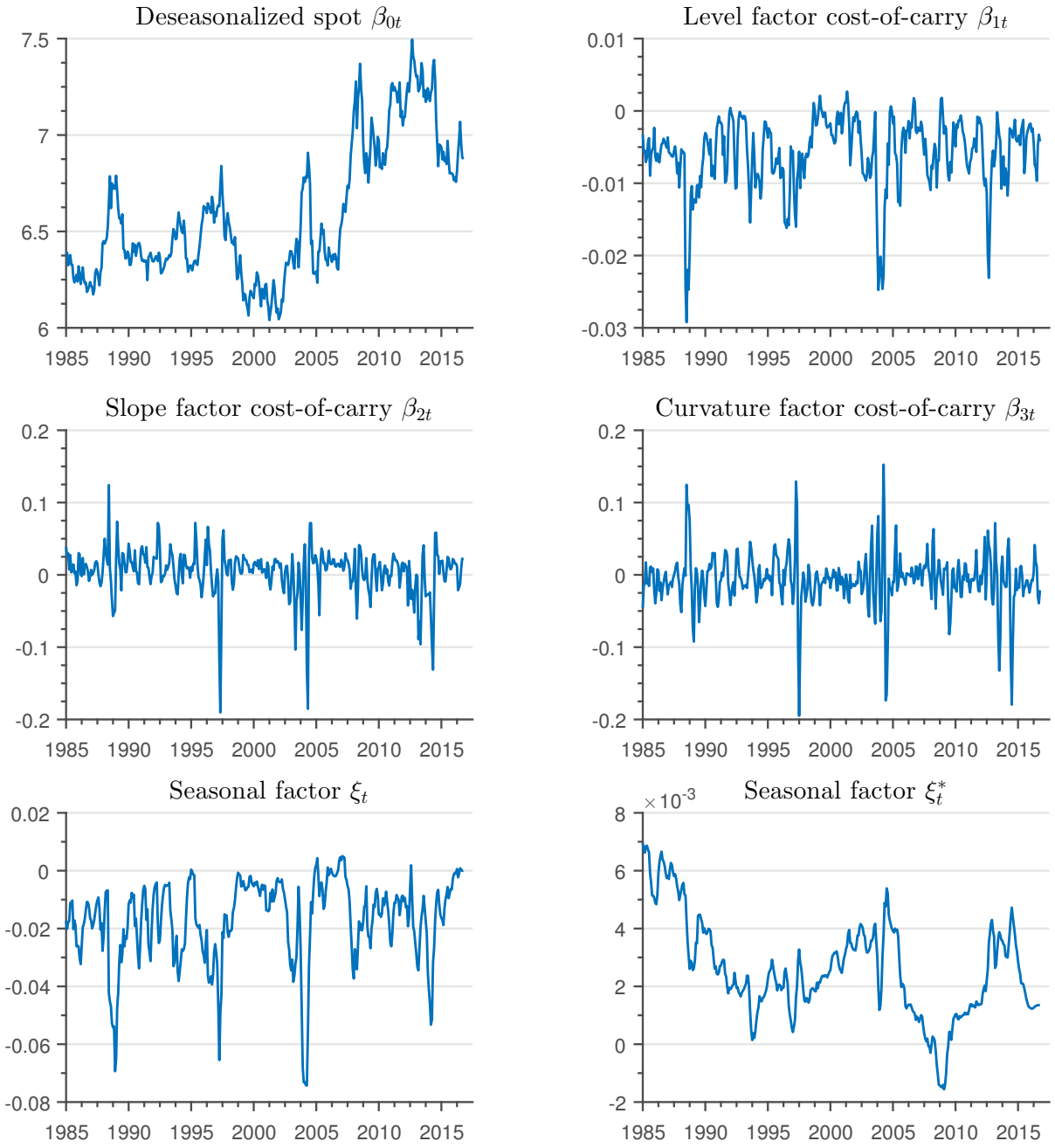

Figure 3: Soybean: Fitted log-futures curves

The figure shows fitted log-futures curves, deseasonalized fitted log-futures curve, and actual log-futures prices on selected dates.

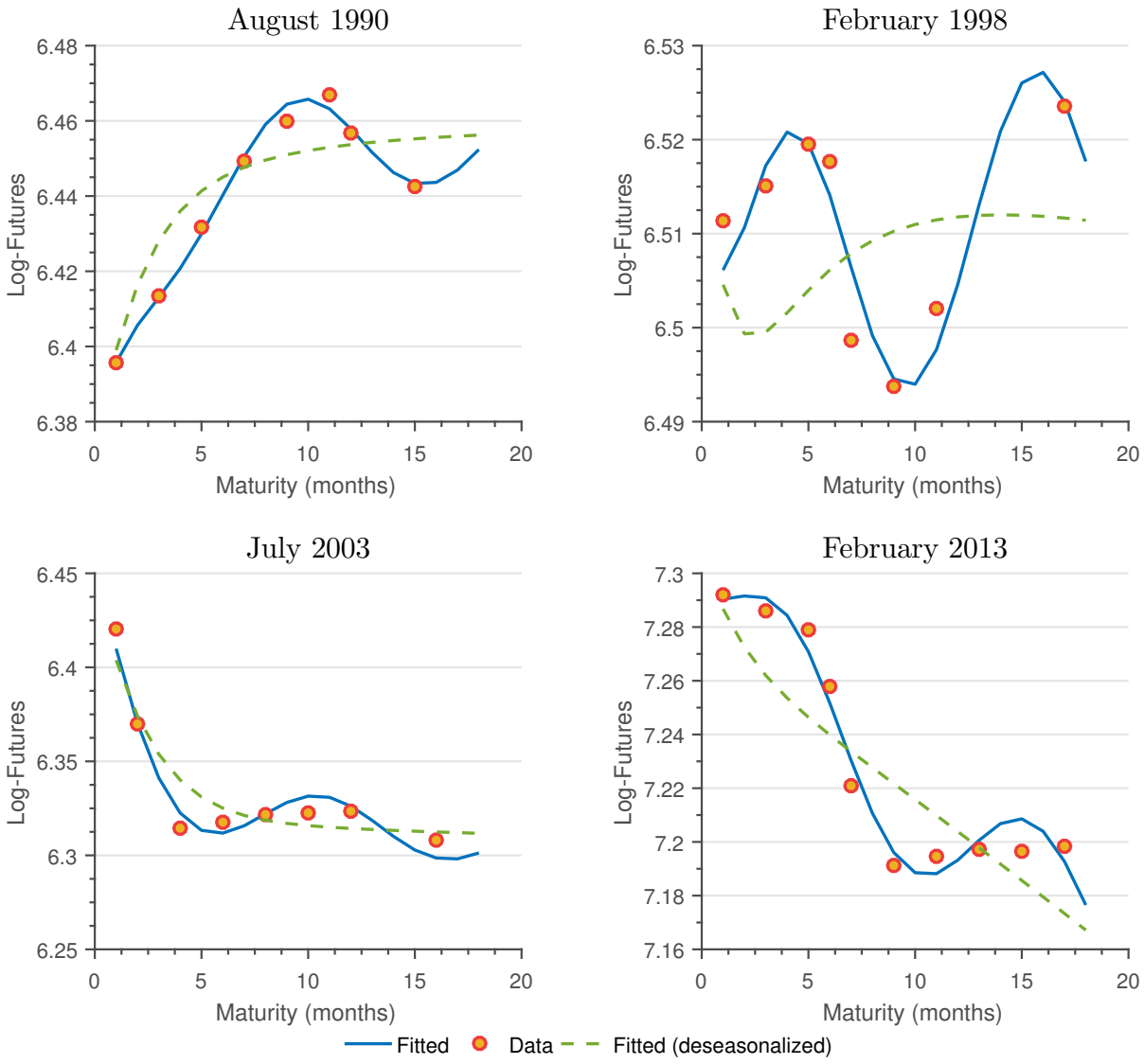

Figure 4: Soybean: Expected 1-month holding futures returns

This figures shows the expected 1-month holding returns of a 1-month and a 18-months futures contract. Returns are expressed in percentage points and on an annualized basis. The upper left panel displays the total expected return. The other panels display the contribution of the different factors. The upper right panel also shows the negative of the level factor of the interest rates and the bottom left panel adds the level of the cost-of-carry factor.

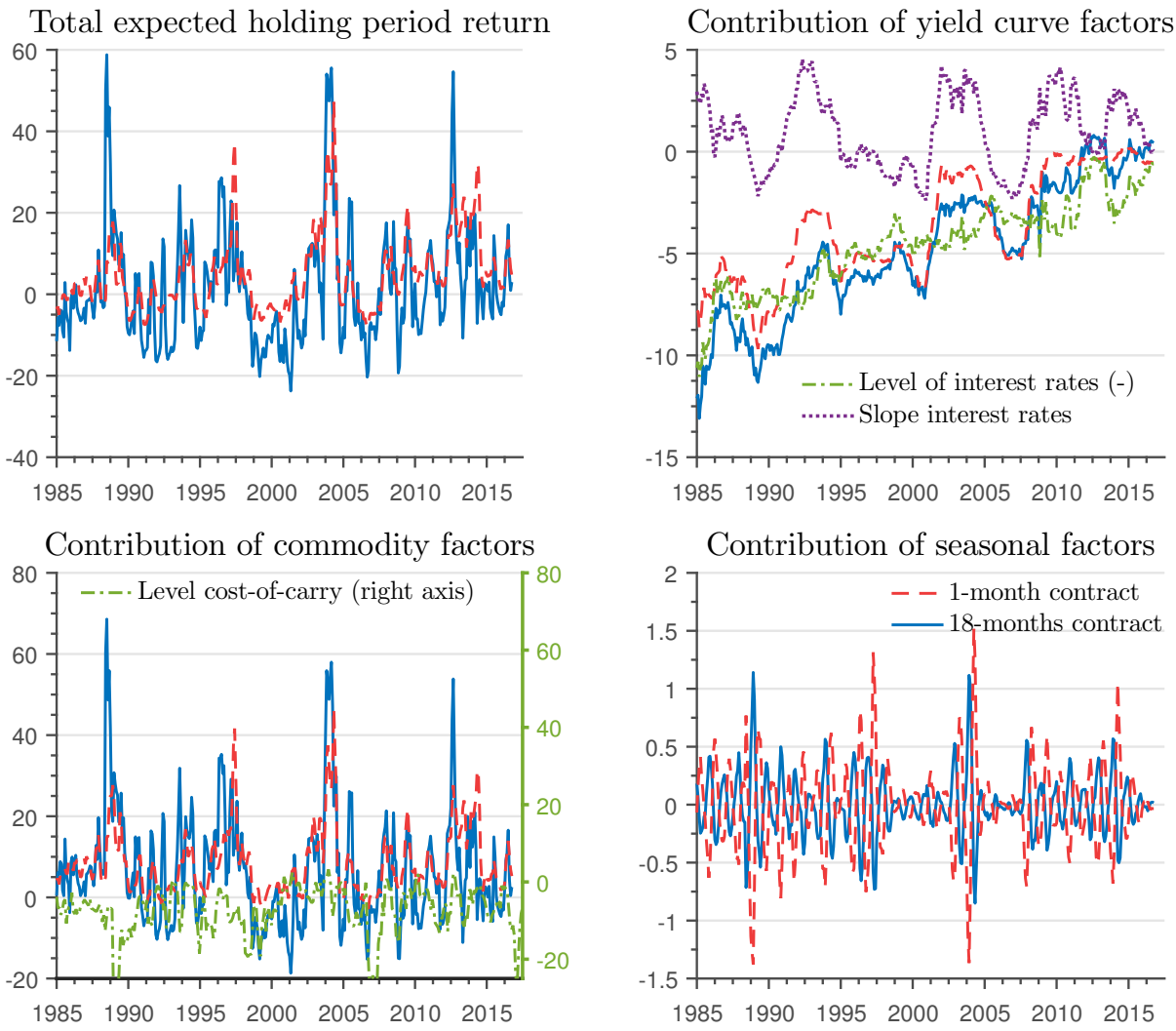

Figure 5: Soybean: Expected holding futures returns of an 18-month futures contract

Expected 1-month and 18-months holding returns of an 18-months futures contract. Returns are expressed in percentage points and on an annualized basis. The upper left panel displays the total expected return. The other panels display the contribution of the different factors. The upper right panel also shows the negative of the level factor and the slope of the interest rates and the bottom left panel adds the commodity spot factor.

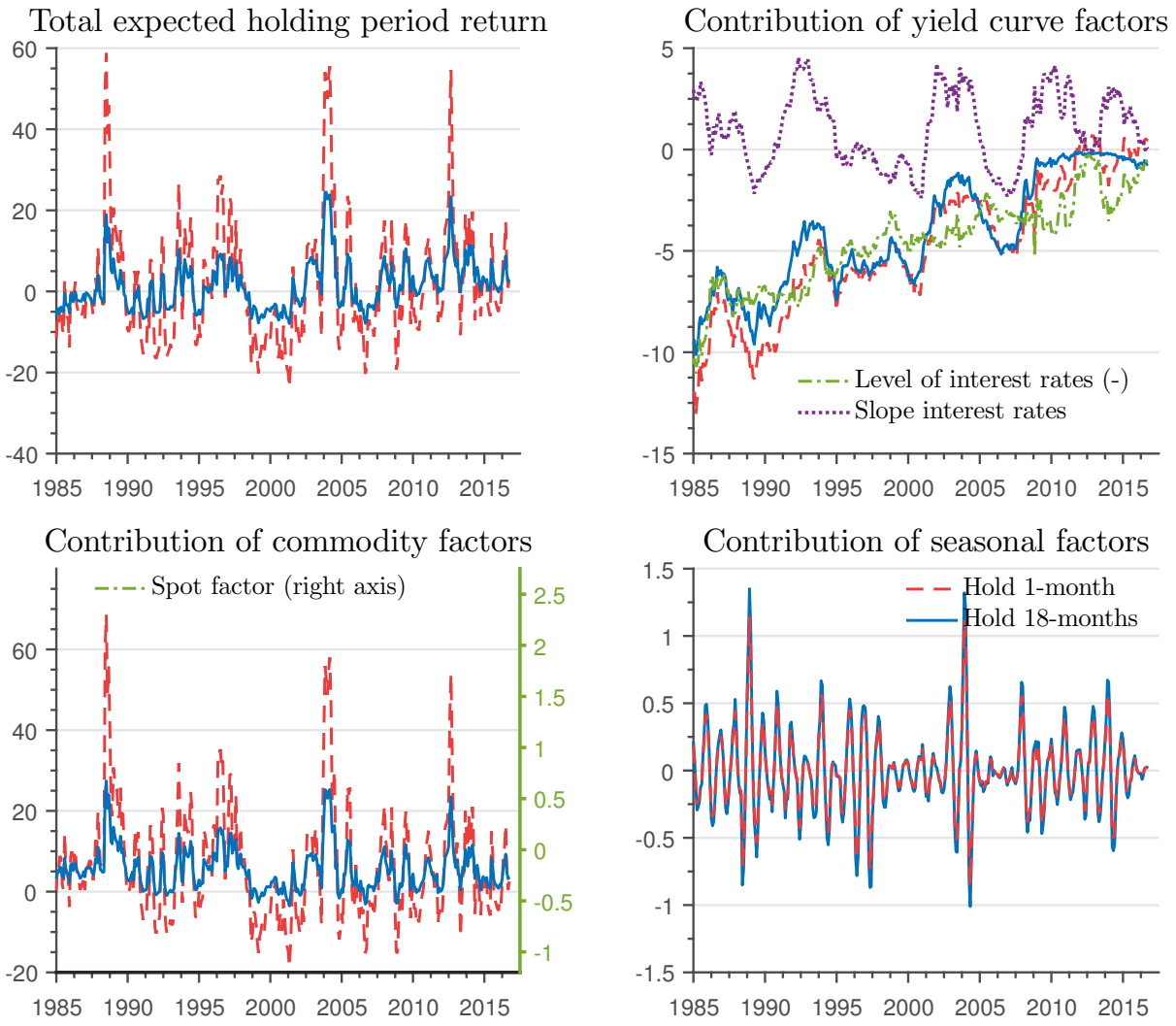

F The zero lower bound on interest rates

This section describes the model that we use to estimate futures prices and bond yields respecting the zero lower bound constraint on interest rates. The model is similar to that described in Section 3 of the paper but replacing the interest rate process $r_t = \rho_0 + \rho_1 X_t$ by an affine shadow interest rate of the form

$$z_t = \rho_0 + \rho_1' X_t. \tag{1}$$

The short term interest rate is is given by

$$r_t = \max(z_t, \underline{r}). \tag{2}$$

The evolution of the state variables under the physical and risk neutral measure are,

$$X_{t+1} = \mu + \Theta X_t + \Gamma \eta_{t+1}, \tag{3}$$

$$X_{t+1} = \mu^Q + \Theta^Q X_t + \Gamma \eta^Q_{t+1}, \tag{4}$$

where $\eta_{t+1} \sim N(0, I)$, $\eta^Q_{t+1} \sim N(0, I)$, and Γ is lower triangular.

This modification renders the model non-linear. While we could approximate the solution using numerical techniques, estimating the parameters becomes challenging because each evaluation of the likelihood function requires numerically solving the model and performing an non-linear filtering procedure. Instead, we adapt the methodology proposed by Wu and Xia (2016).

To find bond prices it is convenient to compute forecasts of the state variables and the shadow rate under both, the physical and risk neutral measure. The conditional expectation

and conditional variance of X_{t+j} under the physical measure are given by

$$X_{t+n} = \left(\sum_{j=0}^{n-1} \Theta^j \right) \mu + \Theta^n X_t + \sum_{j=0}^{n-1} \Theta^j \Gamma \eta_{t+n-j}.$$

Therefore,

$$\begin{aligned} E_t \left(X_{t+n} | X_t \right) &= \left(\sum_{j=0}^{n-1} \Theta^j \right) \mu + \Theta^n X_t \\ Var_t \left(X_{t+n} | X_t \right) &= \sum_{j=0}^{n-1} \Theta^j \Gamma \Gamma' \Theta'^j \end{aligned}$$

Under the risk-neutral measure the moments are

$$\begin{aligned} E_t^Q \left(X_{t+n} | X_t \right) &= \left(\sum_{j=0}^{n-1} \left(\Theta^Q \right)^j \right) \mu^Q + \left(\Theta^Q \right)^n X_t \\ Var_t^Q \left(X_{t+n} | X_t \right) &= \sum_{j=0}^{n-1} \left(\Theta^Q \right)^j \Gamma \Gamma' \left(\Theta^{Q\prime} \right)^j \end{aligned}$$

Therefore, the conditional mean and variance of the shadow rate z_{t+n} under the risk neutral measure are

$$\begin{aligned} E_t^Q \left[z_{t+n} | X_t \right] =& \rho_0 + \rho_1' E_t^Q \left[X_{t+n} | X_t \right] \\ =& \rho_0 + \rho_1' \left[\left(\sum_{j=0}^{n-1} \left(\Theta^Q \right)^j \right) \mu^Q + \left(\Theta^Q \right)^n X_t \right] \\ =& \rho_0 + \rho_1' \left(\sum_{j=0}^{n-1} \left(\Theta^Q \right)^j \right) \mu^Q + \rho_1' \left(\Theta^Q \right)^n X_t \end{aligned}$$

$$\begin{aligned}\left(\sigma_n^Q\right)^2 =& Var_t^Q\left(z_{t+n}|X_t\right)\\ =& Var_t^Q\left(\rho_0+\rho_1' X_{t+n}|X_t\right)\\ =& \rho_1' Var_t^Q\left(X_{t+n}|X_t\right)\rho_1\\ =& \rho_1'\left(\sum_{j=0}^{n-1}\Theta^{Qj}\Gamma\Gamma'\Theta^{Q\prime j}\right)\rho_1.\end{aligned}$$

We will use these moments later. Let's define some notation first,

$$\begin{aligned}\bar{a}_n =& \rho_0+\rho_1'\left(\sum_{j=0}^{n-1}\left(\Theta^Q\right)^j\right)\mu^Q\\ \tilde{a}_n =& \bar{a}_n-\frac{1}{2}\rho_1'\left(\sum_{j=0}^{n-1}\left(\Theta^Q\right)^j\right)\Gamma\Gamma'\left(\sum_{j=0}^{n-1}\left(\Theta^Q\right)^j\right)'\rho_1\\ \tilde{b}_n' =& \rho_1'\left(\Theta^Q\right)^n\\ \left(\sigma_n^Q\right)^2 =& \rho_1'\left(\sum_{j=0}^{n-1}\left(\Theta^Q\right)^j\Gamma\Gamma'\left(\Theta^{Q\prime}\right)^j\right)\rho_1\end{aligned}$$

so that

$$\begin{aligned}E_t^Q\left[z_{t+n}|X_t\right] =& \bar{a}_n+\tilde{b}_n' X_t\\ Var_t^Q\left(z_{t+n}|X_t\right) =& \left(\sigma_n^Q\right)^2.\end{aligned}$$

and

$$\frac{1}{2}\left(Var_t^Q\left(\sum_{j=0}^{n}z_{t+j}\right)-Var_t^Q\left(\sum_{j=0}^{n-1}z_{t+j}\right)\right)=\bar{a}_n-\tilde{a}_n.$$

Pricing government bonds imposing the zero lower bound on interest rates

The price of a zero coupon bond satisfies

$$P_t^{(n)}=E_t^Q\left(e^{-\sum_{j=0}^{n-1}r_{t+j}}\right)=e^{-r_t}E_t^Q\left(e^{-\sum_{j=1}^{n-1}r_{t+j}}\right)$$

so that

$$p_t^{(n)} = -r_t + \log E_t^Q \left(e^{-\sum_{j=1}^{n-1} r_{t+j}} \right).$$

Therefore, the (log) forward interest rate $\ell_t^{(n,n+1)}$ is given by

$$\begin{aligned}
\ell_t^{(n,n+1)} =& p_t^{(n)} - p_t^{(n+1)} \\
=& -r_t + \log \left(E_t^Q e^{-\sum_{j=1}^{n-1} r_{t+j}} \right) - \left(-r_t + \log \left(E_t^Q e^{-\sum_{j=1}^{n} r_{t+j}} \right) \right) \\
=& \log \left(E_t^Q e^{-\sum_{j=1}^{n-1} r_{t+j}} \right) - \log \left(E_t^Q e^{-\sum_{j=1}^{n} r_{t+j}} \right).
\end{aligned}$$

Now use the approximation (true for log normal variables) $\log E e^z = E(z) + \frac{1}{2} Var(z)$,

$$\begin{aligned}
\ell_t^{(n,n+1)} \approx& \left(-E_t^Q \sum_{j=1}^{n-1} r_{t+j} + \frac{1}{2} Var_t^Q \left(\sum_{j=1}^{n-1} r_{t+j} \right) \right) - \left(-E_t^Q \sum_{j=1}^{n} r_{t+j} + \frac{1}{2} Var_t^Q \left(\sum_{j=1}^{n} r_{t+j} \right) \right) \\
=& E_t^Q \sum_{j=1}^{n} r_{t+j} - E_t^Q \sum_{j=1}^{n-1} r_{t+j} + \frac{1}{2} Var_t^Q \left(\sum_{j=1}^{n-1} r_{t+j} \right) - \frac{1}{2} Var_t^Q \left(\sum_{j=1}^{n} r_{t+j} \right) \\
=& E_t^Q [r_{t+n}] + \frac{1}{2} \left(Var_t^Q \left(\sum_{j=1}^{n-1} r_{t+j} \right) - Var_t^Q \left(\sum_{j=1}^{n} r_{t+j} \right) \right).
\end{aligned}$$

This expression is exact in a gaussian term structure model. It is an approximation in the model that imposes the zero lower bound on interest rates. We need to solve for these conditional moments. To compute the moments we use properties of truncated normal distribution and an approximation proposed.

$$\begin{aligned}
E_t^Q [r_{t+n}] =& E_t^Q [\max(\underline{r}, z_{t+n})] \\
=& Prob_t^Q (z_{t+n} < \underline{r}) \times \underline{r} + Pr(z_{t+n} \geqslant \underline{r}) \times E_t^Q [z_{t+n} | z_{t+n} \geqslant \underline{r}] \\
=& \underline{r} + \sigma_n^Q \left[\left(\frac{\bar{a}_n + \tilde{b}_n' X_t - \underline{r}}{\sigma_n^Q} \right) \Phi \left(\frac{\bar{a}_n + \tilde{b}_n' X_t - \underline{r}}{\sigma_n^Q} \right) + \phi \left(\frac{\bar{a}_n + \tilde{b}_n' X_t - \underline{r}}{\sigma_n^Q} \right) \right] \\
=& \underline{r} + \sigma_n^Q g \left(\frac{\bar{a}_n + \tilde{b}_n' X_t - \underline{r}}{\sigma_n^Q} \right)
\end{aligned}$$

This is equation (A2) in Wu and Xia (2016). Here Φ and ϕ are the cumulative distribution and density of the standard normal and the function $g(x) = x\Phi(x) + \phi(x)$ for any x.

Wu and Xia (2016) also use the approximation (see page 283)

$$\frac{1}{2}\left(Var_t^Q\left(\sum_{j=1}^{n-1} r_{t+j}\right) - Var_t^Q\left(\sum_{j=1}^{n} r_{t+j}\right)\right) \approx \Phi\left(\frac{\bar{a}_n + \tilde{b}_n' X_t - \underline{r}}{\sigma_n^Q}\right)(\bar{a}_n - \tilde{a}_n).$$

From here, we conclude that the forward interest rate is

$$f_t^{(n,n+1)} \approx \underline{r} + \sigma_n^Q g\left(\frac{\bar{a}_n + \tilde{b}_n' X_t - \underline{r}}{\sigma_n^Q}\right) + \Phi\left(\frac{\bar{a}_n + \tilde{b}_n' X_t - \underline{r}}{\sigma_n^Q}\right) \times (\bar{a}_n - \tilde{a}_n)$$

Using a Taylor expansion, Wu and Xia (2016) conclude

$$f_t^{(n,n+1)} \approx \underline{r} + \sigma_n^Q g\left(\frac{\tilde{a}_n + \tilde{b}_n' X_t - \underline{r}}{\sigma_n^Q}\right). \tag{5}$$

In the model without the zero lower bound, the forward rate is $f_t^{(n,n+1)} = \tilde{a}_n + \tilde{b}_n' X_t$. Note, also that the function $g(x)$ is non-negative, increasing, approaches zero as x decreases, and approaches $g(x) = x$ as x increases. Moreover,

$$g'(x) = \Phi(x) + x\phi(x) + \phi'(x)$$

but using $\phi(x) = \frac{e^{-x^2/2}}{\sqrt{2\pi}}$ so that $\phi'(x) = \frac{e^{-x^2/2}}{\sqrt{2\pi}}(-x) = -x\phi(x)$, it follows that $x\phi(x) + \phi'(x) = 0$ for all x. Therefore,

$$g'(x) = \Phi(x).$$

To estimate the model, Wu and Xia (2016) use as observation equation the forward interest rates. We find it convenient instead to estimate the model using bond yield. Bond

yields and interest rates are related by possible to use actual yields, using the relation

$$y_t^{(\tau)} = \frac{1}{\tau}\sum_{j=0}^{\tau-1} f_t^{(j,j+1)}$$

so that

$$y_t^{(\tau)} = \underline{r} + \frac{1}{\tau}\sum_{j=0}^{\tau} \sigma_j^Q g\left(\frac{\tilde{a}_j + \tilde{b}_j' X_t - \underline{r}}{\sigma_j^Q}\right). \tag{6}$$

That is, the yield is a non-linear function of the factors X_t, which we can write succinctly as $y_t^{(n)} = \mathcal{Y}^{(n)}(X_t)$.

With this notation, the state-space model is given by

$$\begin{aligned}
X_{t+1} &= \mu + \Theta X_t + \Gamma \eta_{t+1} \\
y_t^{(\tau_y)} &= \mathcal{Y}^{(\tau_y)}(X_t) + \varepsilon_{yt}^{(\tau_y)} \\
f_t^{(\tau_f)} &= \beta_{0t} + \tau_f\left(\mathcal{Y}^{(\tau_f)}(X_t) + \tilde{u}_t^{(\tau_f)}\right) + e^{-\omega\tau}\left[\xi_t \cos(\tfrac{2\pi}{12} m_{t+\tau}) + \xi_t^* \sin(\tfrac{2\pi}{12} m_{t+\tau})\right] + \varepsilon_{ft}^{(\tau_f)},
\end{aligned} \tag{7}$$

where $\varepsilon_{yt}^{(\tau_y)}$ and $\varepsilon_{ft}^{(\tau_f)}$ are measurement errors, $\tau_y \in \mathcal{T}_y$, $\tau_f \in \mathcal{T}_f$, and $\tilde{u}_t^{(\tau_f)}$ is given by

$$\tilde{u}_t^{(\tau)} = g_\tau^{m_t} + \beta_{1t} + \left(\frac{1-e^{-\zeta_2\tau}}{\zeta_2\tau}\right)\beta_{2t} + \left(\frac{1-e^{-\zeta_2\tau}}{\zeta_2\tau} - e^{-\zeta_2\tau}\right)\beta_{3t}.$$

F.1 The non-linear state space system and the Extended Kalman Filter

To estimate the parameters of the model, we use the the extended Kalman filter to evaluate the likelihood function. The only non-linear component of the previous system is the mapping from X_t to bond yields, $\mathcal{Y}^{(\tau_y)}$.

We now perform a first order Taylor expansion of $\mathcal{Y}^{(\tau_y)}$ around an arbitrary point $\tilde{X}_t$,

$$\mathcal{Y}^{(\tau)}(X_t) \approx \mathcal{Y}^{(\tau)}(\tilde{X}_t) + \nabla\mathcal{Y}^{(\tau)}(\tilde{X}_t)\left(X_t - \tilde{X}_t\right)$$

The gradient is

$$\nabla \mathcal{Y}^{(\tau)}(\tilde{X}_t) = \left[\frac{\partial \mathcal{Y}^{(\tau)}(\tilde{X}_t)}{\partial X_{1,t}}, \frac{\partial \mathcal{Y}^{(\tau)}(\tilde{X}_t)}{\partial X_{2,t}}, ..., \frac{\partial \mathcal{Y}^{(\tau)}(\tilde{X}_t)}{\partial X_{n,t}} \right]'$$

where n is the dimension of X_t. Also, for $k = 1, 2, ..., m$,

$$\begin{aligned}
\frac{\partial \mathcal{Y}^{(\tau)}(\tilde{X}_t)}{\partial X_{k,t}} =& \frac{1}{\tau} \sum_{j=0}^{\tau-1} \sigma_j^Q g' \left(\frac{\tilde{a}_j + \tilde{b}_j' X_t - \underline{r}}{\sigma_j^Q} \right) \frac{\tilde{b}_{j,k}}{\sigma_j^Q} \\
=& \frac{1}{\tau} \sum_{j=0}^{\tau-1} g' \left(\frac{\tilde{a}_j + \tilde{a}_j' X_t - \underline{r}}{\sigma_j^Q} \right) \tilde{b}_{j,k} \\
=& \frac{1}{\tau} \sum_{j=0}^{\tau-1} \Phi \left(\frac{\tilde{a}_j + \tilde{b}_j' X_t - \underline{r}}{\sigma_j^Q} \right) \tilde{b}_{j,k}
\end{aligned}$$

where $\tilde{b}_{j,k}$ is element k of the vector b_j and $g'(x) = \Phi(x)$. Therefore,

$$\begin{aligned}
\nabla \mathcal{Y}^{(\tau)}\left(\tilde{X}_t\right) =& \left[\frac{\partial \mathcal{Y}^{(\tau)}\left(\tilde{X}_t\right)}{\partial X_{1,t}}, \frac{\partial \mathcal{Y}^{(\tau)}\left(\tilde{X}_t\right)}{\partial X_{2,t}}, ..., \frac{\partial \mathcal{Y}^{(\tau)}\left(\tilde{X}_t\right)}{\partial X_{n,t}} \right] \\
=& \frac{1}{\tau} \sum_{j=0}^{\tau-1} \Phi \left(\frac{\tilde{a}_j + \tilde{b}_j' X_t - \underline{r}}{\sigma_j^Q} \right) \left[\tilde{b}_{j,1},\ \tilde{b}_{j,2}, ..., \tilde{b}_{j,m} \right] \\
=& \frac{1}{\tau} \sum_{j=0}^{\tau-1} \underbrace{\Phi \left(\frac{a_j + b_j' X_t - \underline{r}}{\sigma_j^Q} \right)}_{1 \times 1} \times \underbrace{\mathbf{b}_j'}_{1 \times m}
\end{aligned}$$

because $\sum_{j=0}^{\tau-1} \Phi \left(\frac{\tilde{a}_j + \tilde{b}_j' X_t - \underline{r}}{\sigma_j^Q} \right)$ is the same for all partial derivatives.

Now suppose that we stack all the yield observations into a vector

$$\mathbf{y}_t = \boldsymbol{\mathcal{Y}}\left(X_t\right) + \boldsymbol{\varepsilon}_{yt}$$

where $\mathbf{y}_t = \left[y_t^{(\tau_1)}, y_t^{(\tau_2)}, ..., y_t^{(\tau_m)} \right]'$, $\boldsymbol{\mathcal{Y}}\left(X_t\right) = \left[\mathcal{Y}^{(\tau_1)}\left(X_t\right), \mathcal{Y}^{(\tau_2)}\left(X_t\right), ..., \mathcal{Y}^{(\tau_m)}\left(X_t\right) \right]'$ and

$\varepsilon_{yt} = \left[\varepsilon_t^{(\tau_1)}, \varepsilon_t^{(\tau_2)}, ..., \varepsilon_t^{(\tau_m)}\right]'$. Then the Taylor approximation around $X_t = \tilde{X}_t$ is

$$y_t \approx \boldsymbol{\mathcal{Y}}\left(\tilde{X}_t\right) + J_{\mathcal{Y}}\left(\tilde{X}_t\right)\left(X_t - \tilde{X}_t\right)$$

and $J_{\mathcal{Y}}\left(\tilde{X}_t\right)$ is the Jacobian matrix of partial derivatives of $\boldsymbol{\mathcal{Y}}\left(X_t\right)$,

$$J_{\mathcal{Y}}\left(\tilde{X}_t\right) = \begin{bmatrix} \frac{\partial \mathcal{Y}^{(\tau_1)}\left(\tilde{X}_t\right)}{\partial X_{1,t}} & \frac{\partial \mathcal{Y}^{(\tau_1)}\left(\tilde{X}_t\right)}{\partial X_{2,t}} & \cdots & \frac{\partial \mathcal{Y}^{(\tau_1)}\left(\tilde{X}_t\right)}{\partial X_{n,t}} \\ \frac{\partial \mathcal{Y}^{(\tau_2)}\left(\tilde{X}_t\right)}{\partial X_{1,t}} & \frac{\partial \mathcal{Y}^{(\tau_2)}\left(\tilde{X}_t\right)}{\partial X_{2,t}} & & \frac{\partial \mathcal{Y}^{(\tau_2)}\left(\tilde{X}_t\right)}{\partial X_{n,t}} \\ \vdots & & \ddots & \vdots \\ \frac{\partial \mathcal{Y}^{(\tau_m)}\left(\tilde{X}_t\right)}{\partial X_{1,t}} & \frac{\partial \mathcal{Y}^{(\tau_m)}\left(\tilde{X}_t\right)}{\partial X_{2,t}} & \cdots & \frac{\partial \mathcal{Y}^{(\tau_m)}\left(\tilde{X}_t\right)}{\partial X_{n,t}} \end{bmatrix}.$$

But using that $\nabla \mathcal{Y}^{(\tau)}\left(\tilde{X}_t\right) = \frac{1}{\tau}\sum_{j=0}^{\tau} \Phi\left(\frac{\tilde{a}_j + \tilde{b}_j' X_t - \underline{r}}{\sigma_j^Q}\right)\tilde{b}_j'$ we have

$$J_{\mathcal{Y}}\left(\tilde{X}_t\right) = \begin{bmatrix} \frac{1}{\tau_1}\sum_{j=0}^{\tau_1 - 1} \Phi\left(\frac{\tilde{a}_j + \tilde{b}_j' X_t - \underline{r}}{\sigma_j^Q}\right)\tilde{b}_j' \\ \frac{1}{\tau_2}\sum_{j=0}^{\tau_2 - 1} \Phi\left(\frac{\tilde{a}_j + \tilde{b}_j' X_t - \underline{r}}{\sigma_j^Q}\right)\tilde{b}_j' \\ \vdots \\ \frac{1}{\tau_m}\sum_{j=0}^{\tau_m - 1} \Phi\left(\frac{\tilde{a}_j + \tilde{b}_j' X_t - \underline{r}}{\sigma_j^Q}\right)\tilde{b}_j' \end{bmatrix}.$$

Let us now stack all yield and commodity futures observations into a vector $Z_t = [y_t', f_t']'$ and measurement errors as $\varepsilon_t = [\varepsilon_{yt}', \varepsilon_{ft}']'$. Then, write the state space system as

$$\begin{aligned} X_{t+1} &= \mu + \Theta X_t + \Gamma \eta_{t+1} \\ Z_t &= \boldsymbol{\mathcal{H}}(X_t) + \varepsilon_t \end{aligned} \tag{8}$$

where function $\boldsymbol{\mathcal{H}}(X_t)$ is appropriately defined using the state-space system (7).

The extended Kalman Filter Consider the state space model 8. Let $\hat{X}_{t|s} = E\left[X_t | Y^s\right]$ where $Z^s = [Z_1, Z_2, ..., Z_s]$ is the history of observations up to time s. The extended Kalman filter

is constructed using the following algorithm

Suppose that we have computed the filtered estimates at time t,

$$\hat{X}_{t|t} = E\left[X_t|Z^t\right], \quad \hat{P}_{t|t} = E\left((X_t - \hat{X}_{t|t})(X_t - \hat{X}_{t|t})'|Z^t\right).$$

Prediction step: Our objective is to compute the $\hat{X}_{t+1|t}$, $\hat{P}_{t+1|t}$, and the prediction of the measurement equation. Using the state equation

$$\begin{aligned} E\left[X_{t+1}|Z^t\right] =& \mu + \Theta E\left[X_t|Z^t\right] \\ \hat{X}_{t+1|t} =& \mu + \Theta \hat{X}_{t|t} \end{aligned}$$

The covariance matrix of this prediction is

$$\begin{aligned} E\left(\left(X_{t+1} - \hat{X}_{t+1|t}\right)\left(X_{t+1} - \hat{X}_{t+1|t}\right)'|Z^t\right) =& E\left(\left(\Theta\left(X_t - \hat{X}_{t|t}\right) + \Gamma\eta_{t+1}\right)\left(\Theta\left(X_t - \hat{X}_{t|t}\right) + \Gamma\eta_{t+1}\right)'|Z^t\right) \\ =& \Theta E\left(\left(X_t - \hat{X}_{t|t}\right)\left(X_t - \hat{X}_{t|t}\right)'|Z^t\right)\Theta' + \Gamma E\left(\eta_{t+1}\eta_{t+1}'|Z^t\right)\Gamma' \\ =& \Theta\hat{P}_{t|t}'\Theta' + \Gamma\Gamma' \end{aligned}$$

Thus,

$$\hat{P}_{t+1|t} = \Theta\hat{P}_{t|t}\Theta' + \Gamma\Gamma'.$$

The prediction of the observation equation is

$$\begin{aligned} E\left[Z_{t+1}|Z^t\right] =& E\left[\mathscr{H}\left(X_{t+1}\right) + \varepsilon_{t+1}|Z^t\right] \\ =& E\left[\mathscr{H}\left(X_{t+1}\right)|Z^t\right] \end{aligned}$$

Now compute a first order Taylor approximation of $\mathscr{H}\left(X_{t+1}\right)$ around the prediction $\hat{X}_{t+1|t}$,

$$\mathscr{H}\left(X_{t+1}\right) \approx \mathscr{H}(\hat{X}_{t+1|t}) + \mathbf{J}_{\mathscr{H}}(\hat{X}_{t+1|t})(X_{t+1} - \hat{X}_{t+1|t})$$

where $\mathscr{H}(\hat{X}_{t+1|t})$ is the Jacobian matrix of $\mathscr{H}(X_t)$ evaluated at $\hat{X}_{t+1|t}$. For the non-linear component of the Jacobian, we use the algebra discussed above. Using this approximation gives

$$\begin{aligned}
E\left[\mathscr{H}(X_{t+1})|Z^t\right] \approx & E\left[\mathscr{H}(\hat{X}_{t+1|t}) + \mathbf{J}_{\mathscr{H}}(\hat{X}_{t+1|t})(X_{t+1} - \hat{X}_{t+1|t})|Z^t\right] \\
= & \mathscr{H}(\hat{X}_{t+1|t}) + \mathbf{J}_{\mathscr{H}}(\hat{X}_{t+1|t})(\hat{X}_{t+1|t} - \hat{X}_{t+1|t}) \\
= & \mathscr{H}(\hat{X}_{t+1|t})
\end{aligned}$$

so that

$$\hat{Z}_{t+1|t} = \mathscr{H}(\hat{X}_{t+1|t}).$$

The innovation is

$$Z_{t+1} - \hat{Z}_{t+1|t} = \mathscr{H}(X_{t+1}) - \mathscr{H}(\hat{X}_{t+1|t}) + \varepsilon_{t+1}$$

Hence, the covariance matrix of the innovation is

$$\begin{aligned}
\Omega_{t+1|t} = & E\left[(Z_{t+1} - \hat{Z}_{t+1|t})(Z_{t+1} - \hat{Z}_{t+1|t})'|Z^t\right] \\
= & E\left[(\mathscr{H}(X_{t+1}) - \mathscr{H}(\hat{X}_{t+1|t})(\mathscr{H}(X_{t+1}) - \mathscr{H}(\hat{X}_{t+1|t})'|Z^t\right] + E\left[\varepsilon_{t+1}\varepsilon_{t+1}'\right] \\
= & E\left[(\mathscr{H}(X_{t+1}) - \mathscr{H}(\hat{X}_{t+1|t})(\mathscr{H}(X_{t+1}) - \mathscr{H}(\hat{X}_{t+1|t})'|Z^t\right] + R
\end{aligned}$$

where $R = E\left[\varepsilon_{t+1}\varepsilon_{t+1}'\right]$. Finally, using the Taylor expansion of $\mathscr{H}(X_{t+1})$ around $\hat{X}_{t+1|t}$,

$$\mathscr{H}(X_{t+1}) - \mathscr{H}(\hat{X}_{t+1|t}) \approx \mathbf{J}_{\mathscr{H}}(\hat{X}_{t+1|t})(X_{t+1} - \hat{X}_{t+1|t})$$

Therefore

$$E\left[(\mathscr{H}(X_{t+1}) - \mathscr{H}(\hat{X}_{t+1|t}))\mathscr{H}(X_{t+1}) - \mathscr{H}(\hat{X}_{t+1|t})'|Z^t\right] \approx \mathbf{J}_{\mathscr{H}}(\hat{X}_{t+1|t})\hat{P}_{t+1|t}\mathbf{J}_{\mathscr{H}}(\hat{X}_{t+1|t})'$$

Hence, the covariance matrix of the innovation is

$$\Omega_{t+1|t} = \mathbf{J}_{\mathscr{H}}(\hat{X}_{t+1|t})\hat{P}_{t+1|t}\mathbf{J}_{\mathscr{H}}(\hat{X}_{t+1|t})' + R.$$

Updating step: Given predictive estimates $\hat{X}_{t+1|t}$ and $\hat{P}_{t+1|t}$, our objective is to find the updated filtered estimates $\hat{X}_{t+1|t+1}$ and $\hat{P}_{t+1|t+1}$. Using the formula for a recursive projection

$$\hat{X}_{t+1|t+1} = \hat{X}_{t+1|t} + \text{proj}(X_{t+1} - \hat{X}_{t+1|t}|Z_{t+1} - Z_{t+1|t})$$

where $\text{proj}(X_{t+1} - \hat{X}_{t+1|t}|Z_{t+1} - Z_{t+1|t})$ is the projection of the prediction error of the state variables $X_{t+1} - \hat{X}_{t+1|t}$ on the prediction error (innovation) of the observed variables $Z_{t+1} - Z_{t+1|t}$. Since the projection is a linear operator,

$$\text{proj}(X_{t+1} - \hat{X}_{t+1|t}|Z_{t+1} - Z_{t+1|t}) = K_t\left(Z_{t+1} - Z_{t+1|t}\right)$$

where the Kalman Gain K_t is

$$K_t = \hat{P}_{t+1|t}\mathbf{J}_{\mathscr{H}}(\hat{X}_{t+1|t})'\Omega^{-1}_{t+1|t}.$$

The Jacobian $\mathbf{J}_{\mathscr{H}}(\hat{X}_{t+1|t})$ and the innovation covariance matrix $\Omega_{t+1|t}$ depend on the state prediction $\hat{X}_{t+1|t}$. Therefore, the updating step of the state equation is

$$\hat{X}_{t+1|t+1} = \hat{X}_{t+1|t} + K_t\left(Z_{t+1} - \hat{Z}_{t+1|t}\right)$$

The covariance matrix of the updating step is

$$\begin{aligned}\hat{P}_{t+1|t+1} =& \hat{P}_{t+1|t} - K_t\Omega_{t+1|t}K_t' \\ =& \left[I - K_t\mathbf{J}_{\mathscr{H}}(\hat{X}_{t+1|t})\right]\hat{P}_{t+1|t}.\end{aligned}$$

Summary of extended Kalman Filter.

Given filtered estimates $\hat{X}_{t|t}$, $\hat{P}_{t|t}$ we compute

Prediction step:

$$\begin{aligned}
\hat{X}_{t+1|t} =& \mu + \Theta \hat{X}_{t|t} \\
\hat{P}_{t+1|t} =& \Theta \hat{P}_{t|t} \Theta' + \Gamma\Gamma' \\
\hat{Z}_{t+1|t} =& \mathcal{H}(\hat{X}_{t+1|t}) \\
\Omega_{t+1|t} =& \mathbf{J}_{\mathcal{H}}(\hat{X}_{t+1|t}) \hat{P}_{t+1|t} \mathbf{J}_{\mathcal{H}}(\hat{X}_{t+1|t})' + R.
\end{aligned}$$

Updating step:

$$\begin{aligned}
K_t =& \hat{P}_{t+1|t} J_H(\hat{X}_{t+1|t})' \Omega^{-1}_{t+1|t}. \\
\hat{X}_{t+1|t+1} =& \hat{X}_{t+1|t} + K_t \left(Z_{t+1} - \hat{Z}_{t+1|t} \right) \\
\hat{P}_{t+1|t+1} =& \left[I - K_t \mathbf{J}_{\mathcal{H}}(\hat{X}_{t+1|t}) \right] \hat{P}_{t+1|t}
\end{aligned}$$

Once we compute the innovations $Z_{t+1} - \hat{Z}_{t+1|t}$ and covariance matrix $\Omega_{t+1|t}$ we evaluate the log-likelihood function as usual.

F.2 Estimates of the model that satisfies the zero lower bound.

To estimate the model we impose the Nelson and Siegel representation of the parameters of the risk neutral measure Θ^Q and μ^Q displayed in Proposition 2 of the paper. Table 5 displays the estimates and Figure 6 shows the commodity factors of the baseline model and the model that imposes the zero lower bound.

Table 5: **Estimates of the model that imposes the zero lower bound on interest rates**
The table shows the estimates of the model using futures prices on heating oil and imposing the zero lower bound on interest rates. The sample period is from January 1983 to April 2017.

Parameters of the VAR(1) process for the yield, the spot and cost-of-carry factors

$\mu_\delta\,(\times 1000)$

$$\begin{bmatrix} 0.284 \\ (0.017) \\ -0.013 \\ (0.026) \\ 0.051 \\ (0.040) \end{bmatrix}$$

$\Theta_{\delta\delta}$

$$\begin{bmatrix} 0.935 & 0.004 & 0.028 \\ (0.004) & (0.009) & (0.004) \\ -0.007 & 0.941 & 0.048 \\ (0.006) & (0.011) & (0.006) \\ -0.006 & 0.044 & 0.935 \\ (0.009) & (0.016) & (0.008) \end{bmatrix}$$

$\Gamma_{\delta\delta}\,(\times 1000)$

$$\begin{bmatrix} 0.332 & 0 & 0 \\ (0.008) & & \\ -0.259 & 0.254 & 0 \\ (0.008) & (0.006) & \\ -0.120 & -0.035 & 0.669 \\ (0.016) & (0.019) & (0.013) \end{bmatrix}$$

$\mu_\beta\,(\times 100)$

$$\begin{bmatrix} -0.0134 \\ (0.9908) \\ -0.0654 \\ (0.0229) \\ -0.01864 \\ (0.4807) \\ 0.5343 \\ (0.3542) \end{bmatrix}$$

$\Theta_{\beta\beta}$

$$\begin{bmatrix} 0.9909 & 0.2165 & 0.9252 & -0.0093 \\ (0.0055) & (0.1893) & (0.0937) & (0.129) \\ 0.0004 & 0.8899 & 0.0153 & 0.020 \\ (0.0001) & (0.096) & (0.002) & (0.002) \\ 0.0001 & -0.5833 & 0.8461 & 0.5303 \\ (0.0021) & (0.1025) & (0.0252) & (0.038) \\ 0.0005 & 1.006 & -0.2248 & 0.3625 \\ (0.0013) & (0.1036) & (0.0259) & (0.036) \end{bmatrix}$$

$\Gamma_{\beta\beta}\,(\times 100)$

$$\begin{bmatrix} 9.549 & 0 & 0 & 0 \\ (0.195) & & & \\ -0.134 & 0.127 & 0 & 0 \\ (0.004) & (0.004) & & \\ -0.981 & -0.005 & 2.743 & 0 \\ (0.047) & (0.045) & (0.134) & \\ -0.088 & -0.290 & -1.88 & 1.062 \\ (0.009) & (0.051) & (0.105) & (0.027) \end{bmatrix}$$

Volatility of seasonal process

$\sigma_\xi = 0.0029\,(0.0001)$ $\quad \sigma_{\xi^*} = 0.0016\,(0.0001)$

Other parameters and log-likelihood

$\zeta_1 = 0.056\,(0.0003)$ $\quad \zeta_2 = 0.396\,(0.008)$ $\quad \omega = 0.0096\,(0.0007)$ $\quad$ Log-likelihood = 42185.81

Figure 6: **Spot, cost-of-carry, and seasonal factors**

Estimates of commodity factors of the baseline model and of the model that imposes the zero lower bound constaint on interest rates.

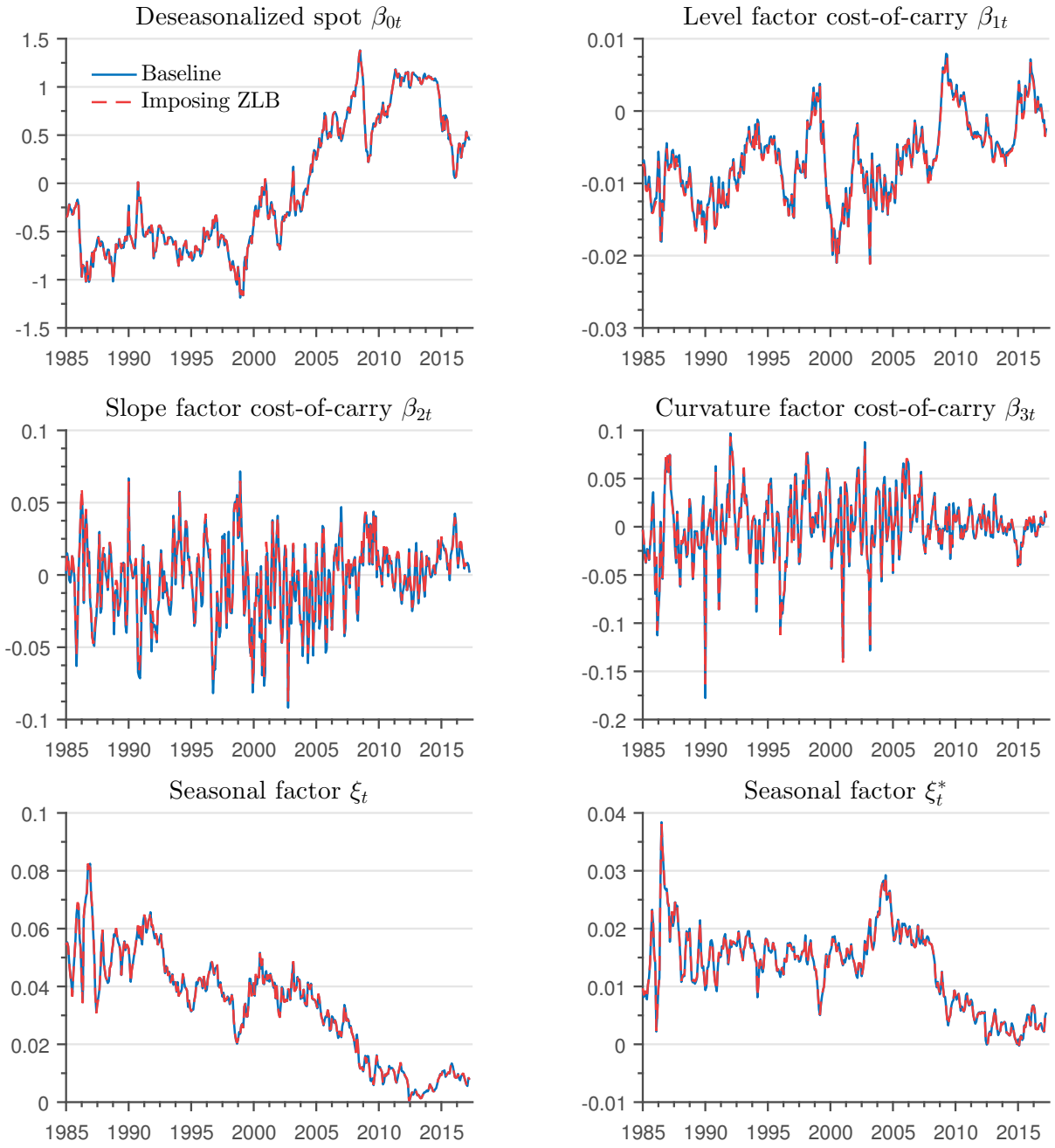

References

Gürkaynak, Refet, Brian Sack, and Jonathan Wright, "The U.S. Treasury yield curve: 1961 to the present," *Journal of Monetary Economics*, 2007, *54* (8), 2291–2304.

Wu, Jing Cynthia and Fan Dora Xia, "Measuring the Macroeconomic Impact of Monetary Policy at the Zero Lower Bound," *Journal of Money, Credit and Banking*, 2016, *48* (2-3), 253–291.